



For Reference

NOT TO BE TAKEN FROM THIS ROOM

COAGULATION AND SURFACE LOSSES
IN DISPERSE SYSTEMS IN STILL AND
TURBULENT AIR

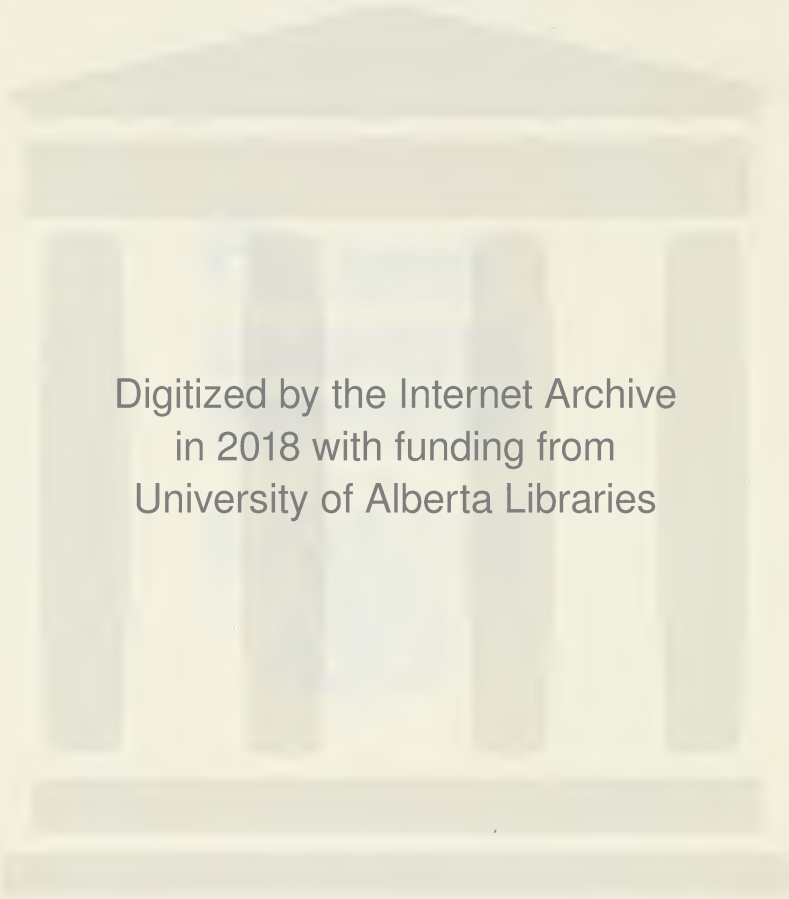
by

Thomas Gillespie, BSc.

University of Alberta, 1947.

Ex LIBRIS
UNIVERSITATIS
ALBERTAENSIS





Digitized by the Internet Archive
in 2018 with funding from
University of Alberta Libraries

<https://archive.org/details/coagulationsurfa00gill>

1937
#35

The undersigned have read and recommend to the Committee on Graduate Studies for acceptance as partial fulfillment for the degree of M.Sc., a thesis submitted by Thomas Gillespie B.Sc. entitled

"COAGULATION AND SURFACE LOSSES IN DISPERSE
SYSTEMS IN STILL AND TURBULENT AIR."

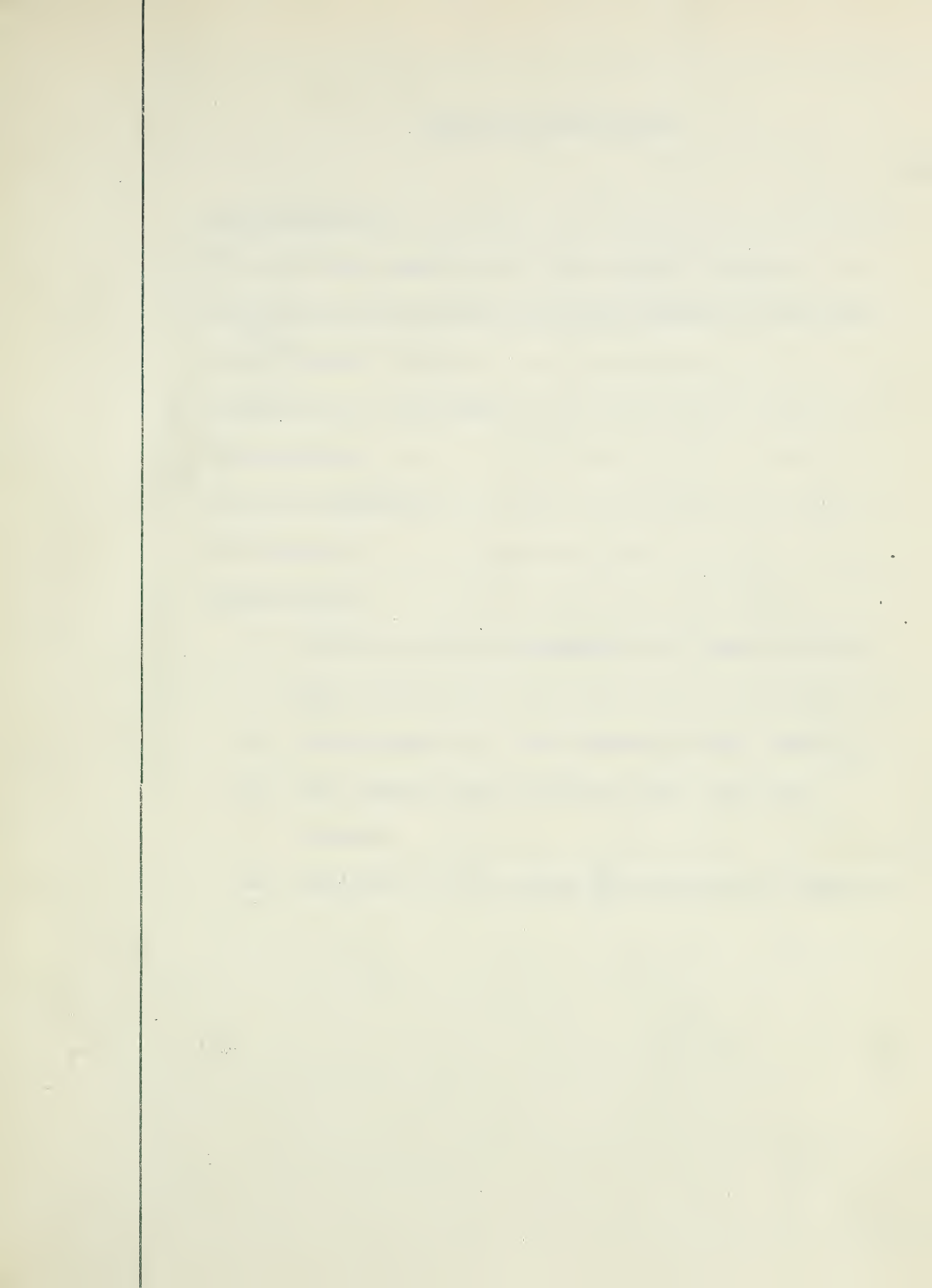


Table of Contents.

	Page.
Introduction.....	1
1. Theoretical Aspects of the Ageing Process.....	4
2. Apparatus, Techniques, and Experimental Procedure..	10
3. Experimental Data.....	29
4. Analysis of the Data.....	34
5. Discussion.....	42
Acknowledgements.....	50
References.....	51
Appendices	
I. Diffusion as a Mechanism of Loss in Still Air.....	52
II. Measurement of the Degree of Air Motion....	54
III. The Coagulation Constant for an Ideal Aerosol.....	62
IV. Analysis of the Mass Concentration Samples.	63

Coagulation and Surface Losses in Disperse Systems
in Still and Turbulent Air.

Extensive studies have been made of the ageing of disperse systems consisting of solid or liquid substances in a finely divided state in ^{still} air, such as smokes, dusts, and fogs. (For general discussions of aerosols see references 13, 15, 16.) It has been found (6, 10, 11, 13, 16) that the increase in particulate volume ($1/n$) with time (t) may be represented by

$$1/n = 1/n_0 + Kt \quad \text{--- (1).}$$

where n denotes the number of particles per c.c. at time t and n_0 that at an early arbitrary time origin. Experimental particle number data given in the literature do not extend beyond ageing times of 100 minutes but it has been stated (10) that the linear relation given by equation (1) holds for intervals as long as 250 minutes. Since equation (1) can be developed on the basis that coagulation is the sole factor responsible for the decrease in particle number of an aerosol with time it has been customary to interpret K as the coagulation constant. It is noteworthy that the values of K determined in this way are considerably greater than that for an ideal aerosol as calculated from a modified form of Smolochowski's theory of coagulating sols (2, 8, 10, 16, also see appendix). Furthermore, constancy of mass concentration is a consequ-

uence of the assumption that coagulation is the sole factor responsible for particle number reduction, and experimentally previous investigators have found this quantity to decrease with time. These two factors indicate ~~that~~ that surface losses are of importance even in still air.

The ageing of aerosols in turbulent air has received comparatively little attention. The results of studies that have been made (4,12) do not lend themselves readily to interpretation in terms of fundamental processes because of the difficulty of translating Tyndall beam brightness data to terms of particle number and size. Except in specially designed laboratory experiments however, problems involving turbulent air conditions are most often encountered.

In a confined space the decrease in particle number of an aerosol is due to coagulation, sedimentation, and loss of these particles which stick to the various surfaces.

In the attempt to obtain a better understanding of the relative importance of these factors, studies have been made of ammonium chloride smoke under various controlled degrees of air motion ranging from the static condition upward. The changes in the mass of dispersed material and the number of particles per c.c. (mass concentration and

particle number) were followed for 330 minutes under each set of conditions. None of the data for these long periods, including the data for still air, could be interpreted on the basis that coagulation was the sole factor responsible for the reduction in particle number. They are described however by equations developed from general postulates involving loss to the surfaces (which includes sedimentation) as well as coagulation. The equations permit an analytical separation of the effects produced by coagulation and loss to adjacent surfaces, and are consistent with fact in the various points for which a comparison has been possible. In particular the equations yield the 'mass loss constant', the 'loss constant', and the coagulation constant descriptive respectively of the decrease in mass of dispersed material, the loss of particles to surfaces, and the loss of particles due to coagulation. Changes in the degree of air motion alter the values of these constants and hence the effect of air motion on the factors involved in the ageing process may be described by plots of the values of the constants vs some index of the degree of air motion. This analysis has been facilitated by the wide range of conditions and the long observation times employed; it would have been difficult to achieve with the data previously reported by other workers for static air conditions and relatively short observation times.

1. Theoretical Aspects of the Ageing Process.

The theoretical considerations of previous investigators on the ageing process are inadequate for our purpose (as shown later) since they do not involve the effect of surface losses. The following considerations which do involve such losses lead to a quantitative description of our experimental data.

An aerosol in turbulent air is brought constantly into contact with various surfaces, and since practically all particles striking a surface stick to it (5, and the present data) there is a consequent decrease in mass concentration and particle number. Under a given set of conditions, the mass of dispersed material that comes into contact with a surface per unit time (and so is lost to the system) should be proportional to the mass concentration m , so that

$$dm/dt = - \alpha m \quad (2)$$

where α denotes the 'mass loss constant'. It follows that

$$\ln (m) = \ln (m_0) - \alpha t \quad (3)$$

over periods for which α may be taken as independent of time; m_0 denotes the mass concentration at time = 0. As will appear later this relation is in agreement with our data and receives strong support from other sources.

Other things being equal, the chance of a particle striking a surface should be proportional to the particle number n , so that the rate of decrease in particle number due to such loss is

$$\left(\frac{dn}{dt}\right)_\ell = - \beta n \text{ --- (4).}$$

where β denotes the 'loss constant'. Since the chance of collision between two particles is proportional to n^2 the rate of decrease of particle number because of coagulation may be written,

$$\left(\frac{dn}{dt}\right)_c = - kn^2 \text{ --- (5).}$$

where k denotes the coagulation constant. It follows that the total rate of decrease in n is given by

$$\left(\frac{dn}{dt}\right) = -(kn^2 + \beta n) \text{ --- (6).}$$

Both k and β may be expected to increase with the degree of air motion because of the increased probability of particle collisions and the increased rate at which the aerosol is brought into contact with surfaces. In addition if an aerosol is confined in a chamber, β should depend upon chamber geometry since a large ratio of wall surface to volume should favor rapid removal of particles. Furthermore, both k and β may be expected to depend to some extent on particle size; the greater mobility of small particles favors a high collision rate, the greater momentum of large particles favors a high loss rate on deflection

of air currents at surfaces, and the greater rate of fall of large particles favors high sedimentation loss. Particle size is subject to change during the ageing of an aerosol, and strictly speaking k and β are in general functions of time.

For intervals over which time variations of k and β may be neglected, it follows on integration of equation (6) that

$$\ln (1/n + k/\beta) = \ln (1/n_0 + k/\beta) + \beta t \quad (7).$$

where n_0 denotes the particle number at $t=0$. As will appear later this expression describes our entire data for a period of 5.5 hours beginning 3 minutes after the generation of the smoke was complete. Equation (7) may be written

$$n = \frac{n_0 e^{-\beta t}}{\phi} \quad (8).$$

$$\text{where } \phi = 1 + (n_0 k/\beta)(1 - e^{-\beta t})$$

The reduction in particle number per c.c. due to surface losses in the interval from 0 to t , denoted by $(\Delta n)_\ell$, can be calculated from equation (4) and (8) as follows:

$$\begin{aligned} (\Delta n)_\ell &= \int_0^t -(\Delta n/\Delta t)_\ell dt = \int_0^t \beta n dt \\ &= \int_0^t \frac{\beta n_0 e^{-\beta t} dt}{1 + (n_0 k/\beta)(1 - e^{-\beta t})} \\ &= (\beta/k) \ln \phi \quad (9a) \end{aligned}$$

The reduction in particle number per c.c. due to coagulation in the interval from 0 to t denoted by $(\Delta n)_c$ is evidently given by

$$\begin{aligned} (\Delta n)_c &= (n_0 - n) - (\Delta n)_l \\ &= (n_0 - n) - (\beta/k) \ln \phi \text{ --- (9b).} \end{aligned}$$

A close relationship may be expected to exist between the loss constant β and the mass loss constant α . If the average mass of the particles in the aerosol and those in lost to surfaces at a given time be denoted by μ and μ' respectively, the mass concentration may be written as $m = \mu n$ and its rate of change as $dm/dt = \mu' (dn/dt)$. Using equations (2) and (4) with these relations it follows that,

$$\begin{aligned} \alpha m &= \mu' \beta n \\ \alpha \mu n &= \mu' \beta n \\ \text{i.e. } \alpha/\beta &= \mu'/\mu \text{ --- (10).} \end{aligned}$$

Hence for a homogeneous aerosol α and β should be equal.

The mechanisms responsible for the observed decrease in mass concentration and particle number in still air may involve sedimentation, diffusion of particles to surfaces, convection currents set up by temperature gradients, and disturbances caused in sampling. Whatever the mechanisms may be it seems reasonable to assume that under given

conditions the loss rate of particles is proportional to n as specified by equation (4), and that the loss rate of mass is proportional to m as specified by equation (2). On this basis equations (2) to (10) should be equally applicable to still or turbulent air conditions. This expectation is borne out by the agreement of experimental data with these equations 2 to 7.

It might be thought at first sight that the mechanisms of loss in still and turbulent air have little in common, since in general, sedimentation velocity is negligibly small compared to the air velocity in turbulence. The former is however superimposed on the latter, and the time average of the latter is zero. Consequently a tendency for material to be deposited most densely on the surface below the aerosol must be expected, and is found in experiments,

Although a sedimentation theory has been worked out for the case of 'non-absorbing' walls (2), it is not applicable in this case since practically all the smoke particles stick to the walls on contact. An idea of the importance of diffusion as a mechanism of loss in still air may be gained from a consideration of the diffusion of homogeneous non-coagulating particles to the 'absorbing walls' of a spherical chamber of radius ρ_0 in the absence of

gravity. It is shown in appendix I that for a uniform initial distribution, the fraction F of the particles remaining after a time t is given by

$$F = \frac{6}{\pi^2} \sum_{\ell} \frac{1}{\ell^2} e^{-\frac{D\pi^2\ell^2 t}{r^2}} \quad \text{--- (11)}$$

where ℓ takes on successive integer values, and the diffusion coefficient D for spherical particles of radius r microns is given (15,2) by

$$D = \frac{10^4 RT}{6\pi \eta r} \left(1 + \frac{A\lambda}{r^2}\right) \quad \text{--- (12)}$$

R, T, N, η, λ , and A denote respectively the gas constant, the absolute temperature, Avogadro's number, the coefficient of viscosity of air, the mean free path of the air molecules, and the Cunningham constant in the correction to Stokes' law. According to these equations the loss by diffusion in a 5 hour period is less than 5% for particles of 0.5 microns radius, and no greater than 10% for particles as small as 0.001 microns in radius. Loss by diffusion therefore seems likely to play only a minor role in the ageing process under laboratory conditions.

The value of the coagulation constant k for an ideal homogeneous aerosol whose spherical particles of r microns radius coagulate on touching may be calculated from the well known expression based on Smolochowski's theory of

coagulating sols (10,16,8,2, see appendix VII)

$$\text{i.e. } k = 1.77 \times 10^{-3} \left(1 + \frac{0.089}{r} \right) \text{ c.c./min.} \quad (13)$$

With regard to neglect of the time dependence of k in the integration leading to equation (7), equation (13) states that in an ideal homogeneous aerosol the variation of k with time is expected to be \rightarrow small once r has attained a value of say 0.5 microns. The predicted increase in k is about 9% when the particle radius increases from 0.5 to 1.0 microns. (In this connection it is of interest to note fig.12 which shows the particle size distributions at different times in the life of NH_4Cl smoke.)

2. Apparatus, Techniques, and Experimental Procedure.

(a) The Smoke Chamber and Stirring Mechanism.

The smoke chamber was a 1.12 meter cube having its internal walls finished with acid-proof paint. A stirrer made of heavy card supported on a light wooden frame and pierced with a series of $5 \times 5 \text{ cm}^2$ holes (fig.1) was mounted centrally on a horizontal axis. To produce the desired degree of air motion it was oscillated through an angle of 130° from the vertical by a motor driven system of gears and shafts. The frequency was determined with the aid of a revolution counter incorporated in the system. This stirring device was used in preference to ord-

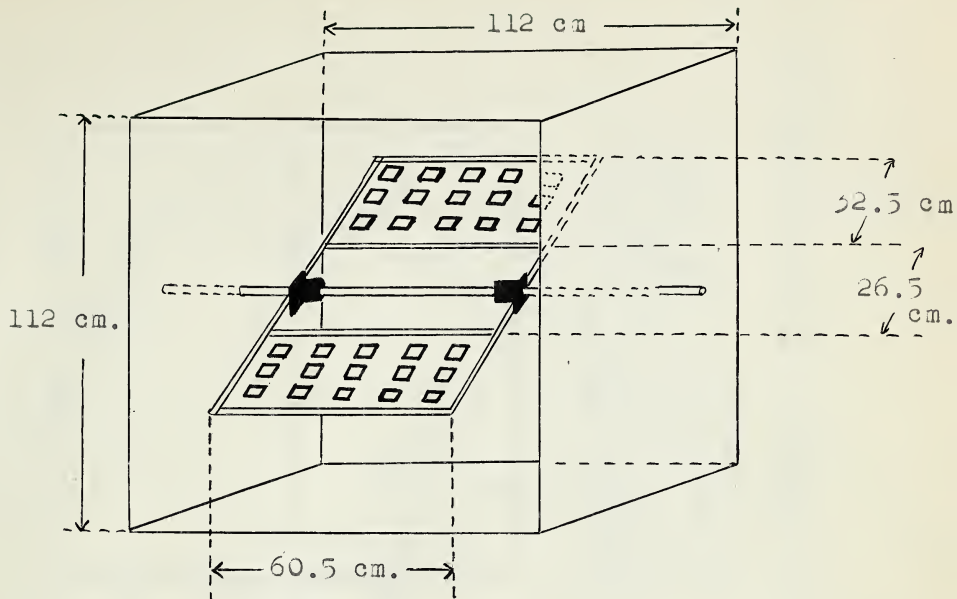


Fig.1: The Smoke Chamber.

inary fans because of its periodic reversal ,its ease of control, and its well defined characteristics as a stirrer.

(b) Specification of the Degree of Air Motion.

The average amount of air passing through a given small volume per unit time regardless of direction was taken as an index of the degree of air motion, although this procedure does not lead to a specification of the degree of turbulence. It is given in terms of the mean air speed (V m/min.) averaged over various points in the chamber (see fig.2.). The characteristics of the air motion with different stirring rates were investigated with

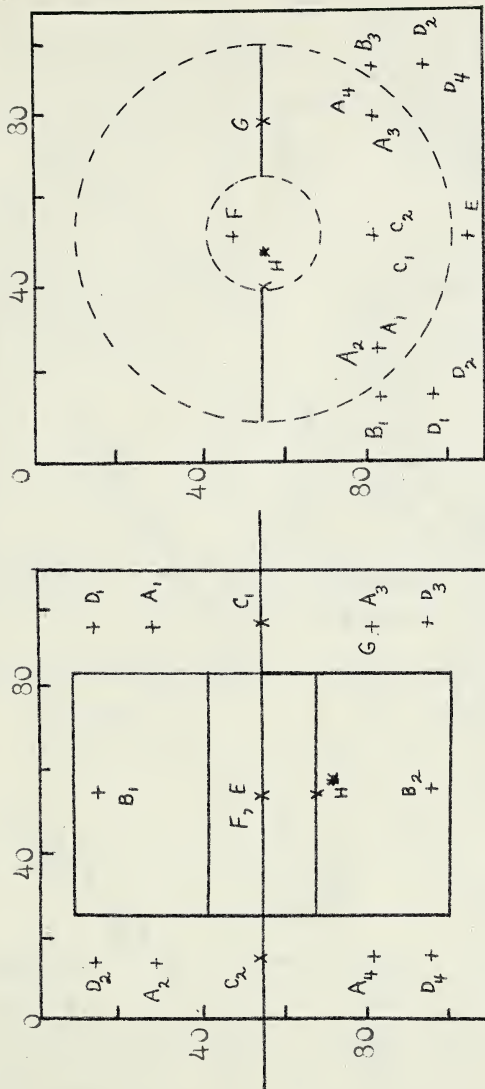


Fig.2(b): Bottom plan of the chamber showing the stirrer in the horizontal position and the location of the points at which the air motion was investigated.

Fig.2(b): End view of the chamber showing the stirrer sweep(circles) and the vertical location of the points at which the air motion was investigated.

* At point H the instrument for measuring the time-average air speed was fastened to the center of the inside edge of the stirrer.

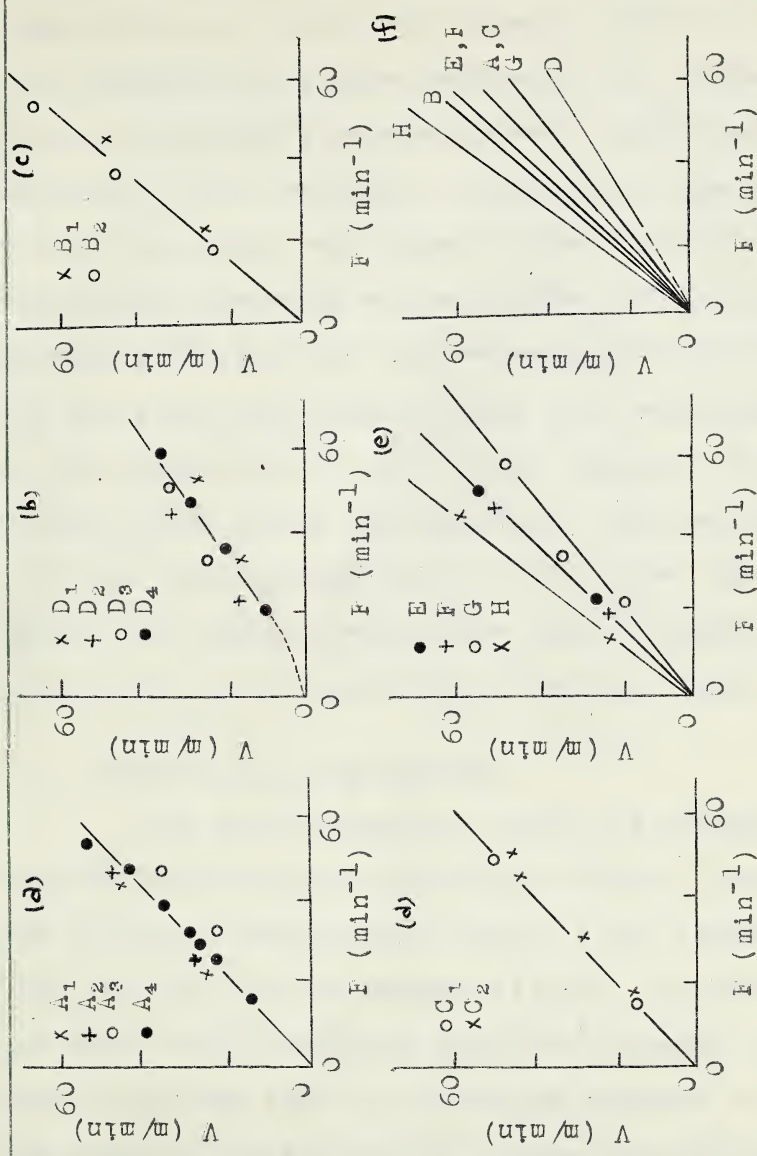


Fig. 2: Plots of V (m/min), the index of air motion vs the frequency of oscillation of the stirrer (min⁻¹).

the aid of of an instrument of the heated thermocouple type developed for the purpose (see appendix III). The time-average air speeds at different points in the chamber determined with this instrument in a series of preliminary experiments were remarkably similar and were proportional to the oscillation frequency of the stirrer (fig.3) except for points very close to the corners. Since the oscillation frequency was maintained constant throughout an experiment, the value of the mean air speed V (m/min.) for the given frequency, averaged over representative points in the chamber, should give a good estimate of the degree of air motion during the experiment. The mean curve for the air speed vs frequency plots of fig.3~~f~~ was used in experiments with smoke to assign the space-average value of V appropriate to the oscillation frequency used.

(c) Production of the Aerosol.

The smoke generator , which was external to the chamber, consisted of a centrifugal blower whose output passed through a control valve into a 7 cm. diameter metal pipe leading into the chamber (fig.4). At the entrance to the pipe a Pitot tube was inserted to permit the adjustment of the air flow to a selected standard value. A 1.5 ohm nichrome heating coil was placed near the exit end of the pipe. A standard amount of NH_4Cl (87 mg.) placed in a

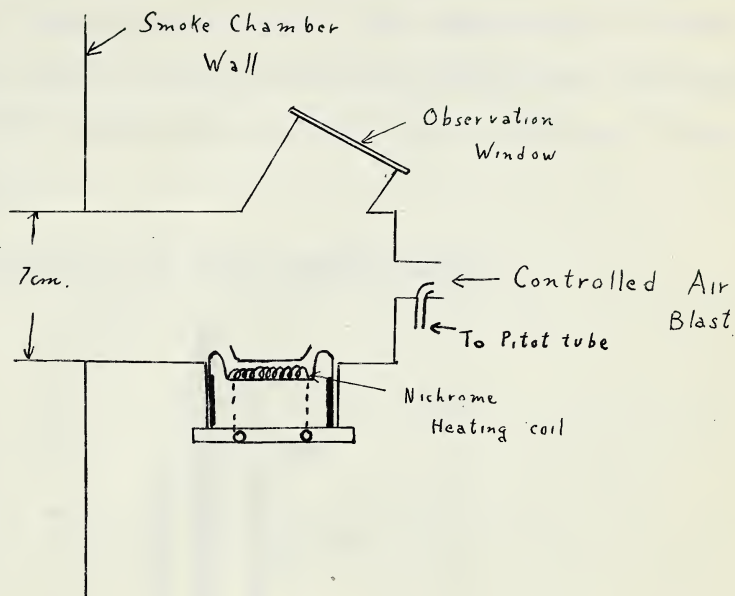


Fig.4. The smoke generator.

pyrex boat on the coil was decomposed in 2 minutes with a heating current of 8.0 amps. A small fan situated within the chamber provided rapid cooling and dilution of the products as they emerged from the exit end of the pipe. The generator was designed with the aim of obtaining a series of aerosols of similar characteristics, for it is known (11,16) that reproducibility is favored with 'blown'

smokes .It is evident that it is essential to obtain such a series of aerosols in order to obtain significant and reproducible results. In our experiments the mass concentration at three minutes after the completion of smoke production varied from 40 to 60 mg./m^3 and the corresponding particle number from 2×10^5 to 4×10^5 c.c.^{-1} (see table III).

(1) Determination of Mass Concentration.

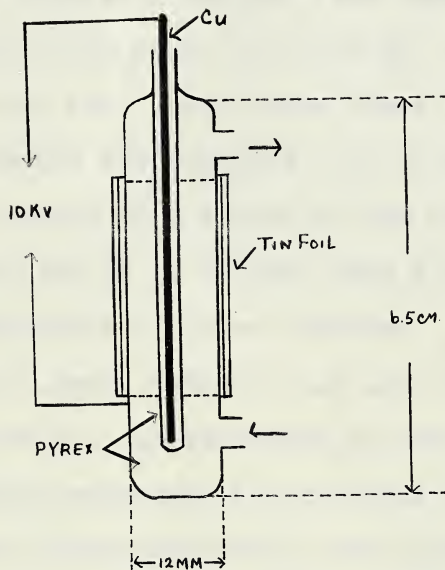


Fig.5: The electrical precipitator.

This quantity was determined from analysis of samples with Messler's reagent. The samples were obtained by electrical precipitation using a modified form of the tube described by Drinker and Hatch (3, see fig.5). The central electrode was enclosed in pyrex to permit thorough cleaning

and to avoid contamination of the sample. In sampling, 500 c.c. of the aerosol were first drawn through the precipitator with no applied voltage by lowering the water level in an attached system. A further volume of 250 c.c. to 4000 c.c. (depending on conditions) was then drawn through with an applied voltage of 10 kv. which produced a discernible glow between the electrodes. The deposit was dissolved in 50 c.c. of distilled water and the resulting solution analysed with Nessler's reagent (see appendix IV). Precipitates ranged from 0.040 to 0.002 mg. of NH_4Cl . Tests carried out with two precipitator tubes in series showed that precipitation was complete i.e. no NH_4Cl could be detected in the second tube either in the early or the late stages of the life of an aerosol when deposits in the first tube were comparable to those obtained in the ageing experiments. For a heavy deposit (1.5 mg.) in the first tube less than 0.005 mg. was deposited in the second tube. The initial flushing procedure was required to obtain a sample representative of the aerosol in the chamber; it did not result in a detectable deposit in the precipitator tube. The total volume taken from the chamber during an experiment by the entire procedure described above was less than 15 liters (i.e. 1.1% of the chamber volume).

(c) Determination of the Number of Particles Per c.c.

The particle number samples were taken with a thermal precipitator (13,7). The precipitator consisted essentially of a shallow rectangular channel, formed by two brass blocks separated by strips of mica. In contact with the brass blocks and resting on the mica strips were placed two discs cut from polished microscope slides. Across the channel and midway between the glass discs was placed a number 32 B and S oxide coated nichrome wire which was heated electrically. The essential parts are shown in figs. 6 and 7. The particles in the aerosol drawn through the precipitator moved rapidly away from the heated wire due to the temperature gradient and were deposited on the glass discs which were kept cool by the brass blocks. The deposits obtained were of suitable density for counting with a high power microscope.


For sampling, the thermal precipitator was mounted on a 2.5 cm. diameter brass tube which extended 10 cms. into the chamber (figs. 6, 7, 8). , 500 c.c. of the aerosol were first drawn through the brass tube from an exit at the precipitator end, and 5 c.c. were then drawn through the cold precipitator by lowering the water level in an attached small bore graduated tube shown in fig. 8. A current of 1.25 amperes was then passed through the precipitator



Fig. 6.The Thermal Precipitator.

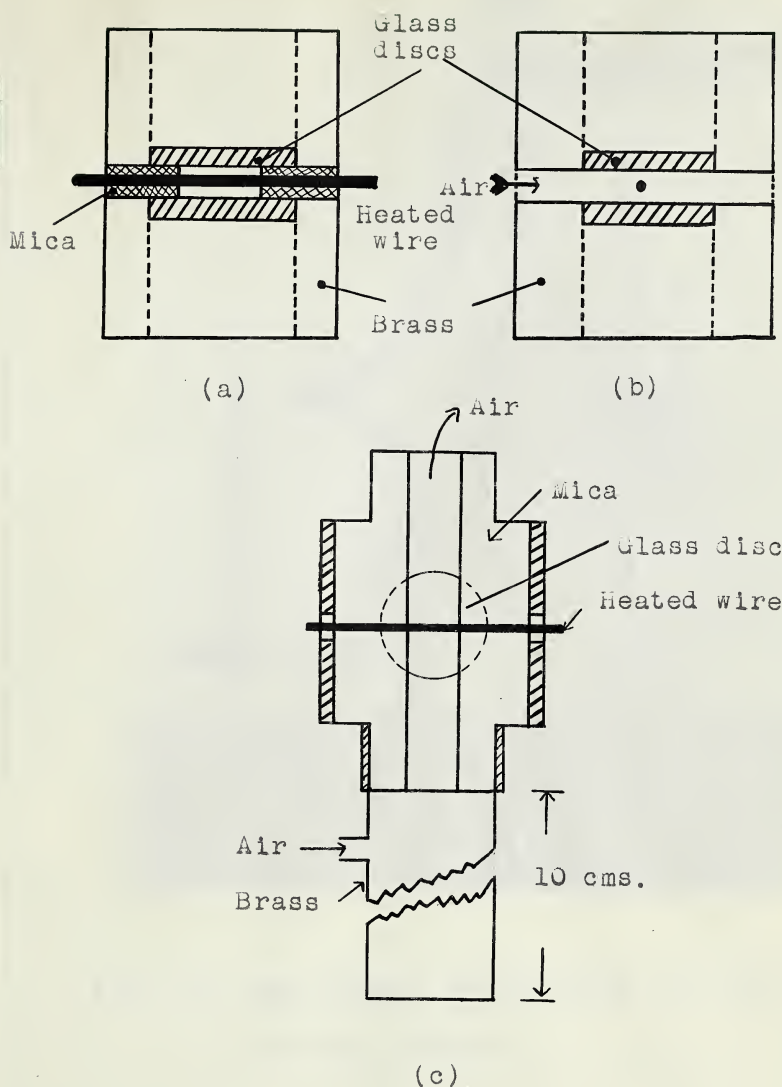


Fig.7: The thermal precipitator. (a) and (b) are respectively the cross and longitudinal sections. (c) is the vertical section parallel to the cover slips.



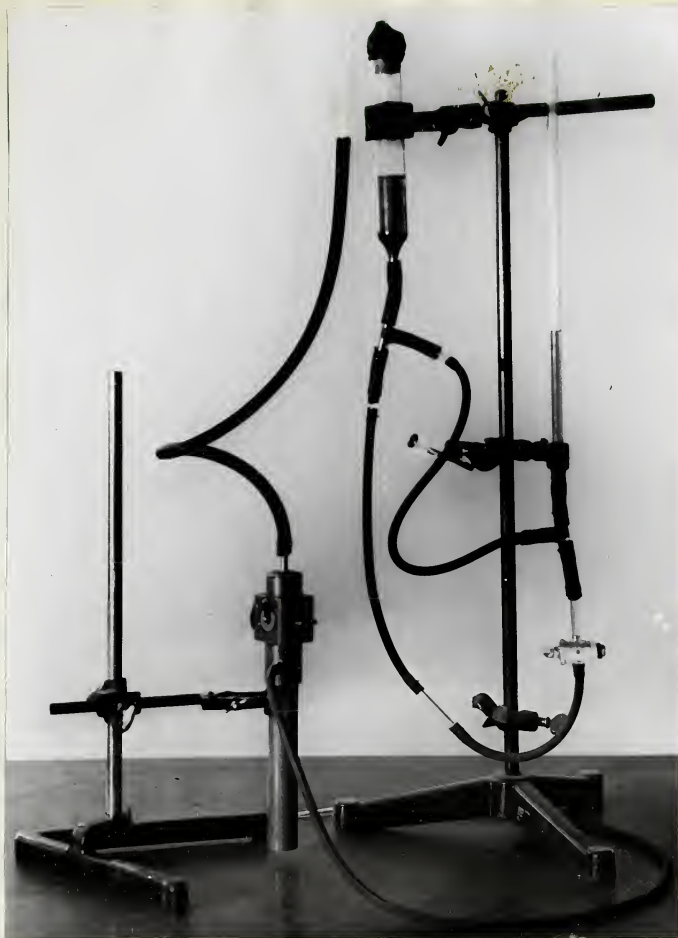


Fig. 8: The thermal precipitator with the attached sampling system.

wire and a further volume of 3.5 c.c. to 10 c.c. (depending on conditions) was drawn through the instrument, starting 5 to 10 seconds after the current had been turned on. The flow rate of 2 to 4 c.c. per minute was well below the value (6.5 c.c./min.) suggested by Green and Watson (7) as an upper limit for efficient operation. Furthermore the deposits formed on the discs had sharp leading edges (fig. 9). This is a characteristic indicative of complete precipitation (7). The initial flushing procedure was required to obtain representative samples. The deposition on the glass discs during ^{this operation} was negligible. Sampling was carried out with the stirring mechanism stationary since preliminary experiments indicated that its motion introduced spurious results. The stoppage interval was not more than one minute for each sample.

The deposits formed on the discs (fig. 9) were 9 mm. long and less than 1 mm. wide. They were examined under a magnification of 440X using darkfield illumination produced by an intense and narrow beam of light approximately normal to the optic axis of the microscope. The light beam was obtained by means of a 110 volt 75 watt projection lamp with a very small filament and a system of lenses and diaphragms. The number of particles in each of 10 equally spaced crosswise strips of width 2.3×10^{-3} cm. was





(a)
(magnification 10X)



(b)
(magnification 100X)

Fig. 9: Portions of typical thermal precipitator deposits. (a) was obtained early in the life of an aerosol (hence composed of small particles) while (b) was taken much later. Since this smoke was allowed to age in still air (b) is composed mainly of large particles. In each case the sharp leading edge is indicative of complete deposition. *(The full length of the deposit is not shown in either case)*

counted for each deposit using a graduated mechanical stage and a Whipple disc in the eyepiece. The known ratio of the examined to the total area of the deposits permitted calculation of the total number of particles deposited, and the number of particles per c.c. was found from this value and the known volume of the sample. The fact that samples taken with no smoke in the chamber gave no visible deposit, ruled out dust as a complicating factor in these experiments.

In some of the earlier experiments aerosol samples were diluted with air before precipitation in order to reduce the particle number and thus facilitate counting. The method of dilution consisted of drawing 350 c.c. of the aerosol into a bell jar containing 3.5 liters of air and mixing with one or two strokes of a stirrer (see Fig. 10). The diluted aerosol was then sampled, and the particulate volume of the original was calculated taking into account the dilution factor. This method gave reliable results as indicated by the data of Fig. 11 for a series of measurements using alternately the direct and dilution method of sampling. Dilution was abandoned on arranging to draw samples of 0.5 to 1.0 c.c. with an accuracy of 3%.



Fig. 10: The apparatus used for diluting very dense aerosols before sampling.

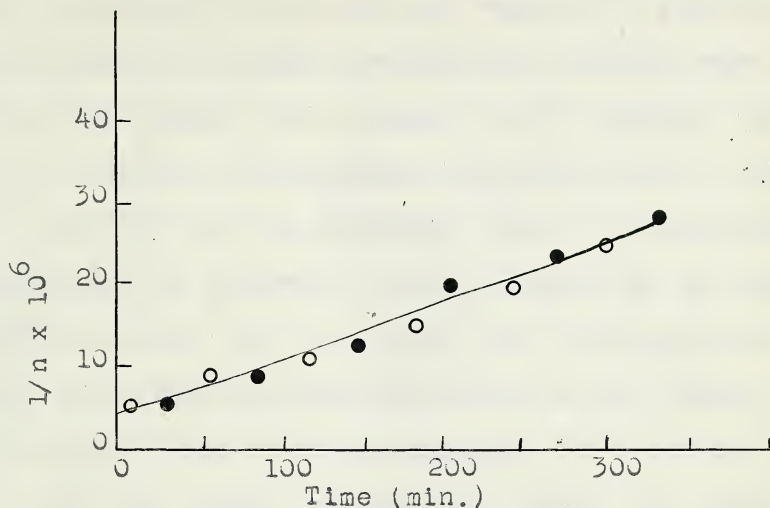


Fig.11: A plot of particulate volumes determined by using the dilution and direct methods of sampling alternately on the same aerosol. The symbols •, and o, refer respectively to 1 cc. samples taken directly and to samples taken by drawing 350 cc. of the aerosol into a 3.5 liter bell jar and mixing with one or two strokes of a stirrer before sampling. (See fig.10). The plotted points are the means of three experiments.

(f) Particle Size Estimation.

Four subsidiary experiments, two with still air and two with a high degree of air motion ($V=50$ m/min.) were performed to provide information on particle size distribution. Thermal precipitator samples were taken every 30 minutes for a period of 280 minutes. The deposits were examined with substage illumination and a magnification of 950X (1.8 mm. objective and a 10 X eyepiece). The particles in crosswise strips selected as for particle number counts were classified into size groups by comparing them with the smallest square in the Whipple disc (projected area 2.2×2.2 microns). If a particle appeared to fill the square its apparent radius was taken to be 1.1 microns. Since this procedure is based on the appearance in two dimensions it may be subject to systematic error. The size groups adopted were; less than 0.3, 0.3-0.6, 0.6-0.9, 0.9-1.1, 1.1-1.4, 1.4-1.7, and 1.7-2.2 microns in apparent radius. In the results shown in fig.12 the number in each size group expressed as a percentage of the total has been plotted at the median radius for the group, that for the first being plotted at 0.2 microns.

(g) The Procedure in Ageing Studies

The generation of smoke was complete within a 2 minute period but the small fan in the chamber was operated

for 3 minutes longer. It was turned off then and the stirrer set in oscillation and maintained at the selected oscillation frequency. All subsequent times were reckoned from a zero set at the moment of turning off the fan. Particle number and mass concentration samples were taken at intervals of 30 mins. for a period of 5.5 hours (see tables I and Ia). Counts were made for the former immediately since dust settling on the glass discs interfered with the counting. Furthermore the apparent number of particles decreased due to deliquescence if the deposits were left for a few hours. The mass concentration samples were usually analysed at any time within a period of 24 hours since the analysis did not change with time if the tubes were well stoppered. The total volume drawn from the chamber during flushing and sampling did not exceed 1.7% of the chamber volume. A series of experiments was performed with various degrees of air motion (see tables I and Ia). After each the chamber was well aired and cleaned.

It was noted that the deposit on the bottom of the chamber was visibly greater than that on the top and side walls under still air conditions. Furthermore, the distribution of the deposit was similar with stirred air, although under this condition the stirrer acquired a deposit comparable to that on the bottom of the chamber.

A series of special experiments was performed to investigate the extent to which particles deposited on the walls were swept off again by the air motion. The procedure was identical with that described above except that all surfaces exposed to the aerosol were coated heavily with oil. Since subsidiary ^{tests} showed that particles striking the the surface were wet immediately it seems reasonable to assume that the return of particles to the aerosol was eliminated in these experiments.

3. Experimental Data.

In tables I and Ia are given particulate volume (V/n) and mass concentration (m) data descriptive of ageing under various degrees of air motion as specified by the index V ($m/min.$). The symbols D38, D40, etc., refer to the serial numbers of experiments. Times (t in minutes) were reckoned from a zero taken 3 minutes after the completion of smoke generation. The values in the columns headed "calc." were obtained from equation (7). In tables II and IIa are given particulate volume and mass concentration data obtained for the experiments in which the chamber walls were wet with oil. It is considered desirable to give the experimental data rather fully since the interpretation differs fundamentally from that given previously by various workers for data covering a more restricted range.

Table I: Particulate volume vs time data for various experiments with different degrees of air motion performed in a chamber with dry walls. The tabulated values are $10^6/n$ cc.

t	V = 0				V = 1.1				V = 5.4				V = 11				V = 22			
	D38		D40		D75		D75		D74		D74		D75		D77		D73		D73	
	obs	calc	obs	calc	obs	calc	obs	calc	obs	calc	obs	calc	obs	calc	obs	calc	obs	calc	obs	calc
0	5.2	5.6	4.8	5.2	-	-	-	-	-	-	-	-	-	-	-	-	-	-	-	-
3	-	-	-	-	2.7	3.6	-	-	2.1	2.9	-	-	3.5	4.4	4.3	4.4	4.3	4.3	-	-
30	6.8	6.8	7.1	6.6	4.3	4.7	-	-	3.6	4.0	-	-	4.9	4.8	6.3	5.8	6.0	6.3	-	-
60	8.3	8.2	7.6	7.9	6.7	6.0	-	-	5.8	5.8	-	-	6.5	6.6	8.2	8.6	9.5	8.8	-	-
90	10.4	9.5	9.5	9.5	8.6	7.6	-	-	7.3	7.7	-	-	8.6	8.9	9.0	9.8	12.1	11.4	-	-
120	-	-	11.4	11.2	9.7	9.4	-	-	10.1	10.0	-	-	11.2	11.5	11.1	12.3	14.3	14.8	-	-
150	-	-	-	-	10.7	11.3	-	-	11.8	12.9	-	-	14.5	15.0	14.0	15.2	19.	19.	-	-
180	14.0	14.6	15.2	15.1	11.9	13.8	-	-	15.7	16.1	-	-	22.	19.	20.	19.	26.	24.	-	-
210	15.8	16.7	17.4	17.7	15.5	17.2	-	-	21.	20.	-	-	25.	24.	22.	23.	31.	29.	-	-
240	19.	19.	21.	20.	19.	19.	-	-	25.	25.	-	-	30.	30.	27.	28.	35.	36.	-	-
270	22.	21.	24.	23.	20.	23.	-	-	29.	30.	-	-	33.	37.	34.	34.	41.	44.	-	-
300	24.	24.	28.	26.	28.	27.	-	-	35.	36.	-	-	46.	46.	43.	42.	59.	54.	-	-
320	-	-	-	-	-	-	-	-	-	-	-	-	57.	53.	-	-	-	-	-	-
325	-	-	-	-	-	-	-	-	-	-	-	-	-	-	-	-	-	-	-	-
330	26.	27.	29.	30.	32.	31.	-	-	43.	44.	-	-	-	-	54.	50.	67.	66.	-	-

Table I (continued)

t	V = 29				V = 35			
	D56		D58		D62		D63	
	obs	calc	obs	calc	obs	calc	obs	calc
0	-	-	-	-	-	-	-	-
2	4.8	4.5	-	-	-	-	-	-
5	-	-	5.1	3.3	5.3	3.3	-	-
30	5.4	6.2	5.4	4.7	5.4	5.0	6.0	6.5
60	10.8	8.5	7.5	7.7	6.8	7.5	9.9	9.5
90	13.2	11.2	8.4	9.1	12.6	11.0	15.9	13.5
120	-	-	12.7	12.3	15.2	15.0	-	-
150	17.4	18.2	16.0	15.8	19.	20.	23.	24.
180	24.	23.	21.	20.	27.	27.	32.	31.
210	29.	29.	27.	26.	34.	36.	43.	41.
240	35.	35.	31.	33.	46.	43.	52.	52.
270	47.	44.	45.	41.	65.	63.	61.	67.
300	54.	54.	52.	52.	82.	82.	79.	85.
320	-	-	-	-	-	-	-	-
325	-	-	61.	62.	-	-	-	-
330	62.	66.	-	-	109.	107.	118.	109.

t	V = 40				V = 50			
	D54		D55		D51		D60	
	obs	calc	obs	calc	obs	calc	obs	calc
0	-	-	-	-	-	-	-	-
2	7.3	5.8	3.6	4.3	4.4	4.0	-	-
5	-	-	-	-	-	-	-	-
30	-	-	9.0	7.3	6.5	7.0	6.0	7.2
60	8.2	11.4	8.5	11.0	12.9	11.5	12.8	11.5
90	16.7	16.3	12.8	15.8	16.3	17.4	23.	18.
120	22.	22.	26.	22.	28.	25.	26.	25.
150	23.	29.	30.	30.	38.	36.	29.	35.
180	54.	39.	43.	40.	53.	50.	43.	49.
210	53.	51.	55.	53.	73.	70.	69.	69.
240	64.	67.	63.	70.	93.	96.	97.	95.
270	88.	89.	92.	93.	128.	129.	-	-
300	115.	113.	125.	123.	176.	176.	164.	176.
325	-	-	-	-	-	-	250.	233.
330	145.	145.	147.	159.	232.	239.	-	-

Table Ia: Mass concentration vs time data for the experiments given in table I. The tabulated values are m in mg/m^3 .

t	V = 0		1.1	5.4	11		22
	D38	D40	D75	D74	D76	D77	D73
10	38.	46.	44.	40.	44.	44.	44.
40	38.	44.	38.	33.	33.	-	35.
70	32.	38.	35.	26.	23.	25.	25.
100	26.	34.	27.	20.	19.	20.	17.
130	24.	37.	30.	13.	15.	15.	12.5
160	20.	32.	18.	15.	14.	15.	12.0
190	18.	25.	17.	12.5	10.	10.	8.0
220	23.	20.	14.	10.	6.7	7.	5.2
250	19.	25.	13.	10.	5.	6.7	6.0
280	17.	21.	13.	8.	4.	5.	3.3
310	14.6	20.	-	-	-	-	-

t	V = 29		35		40		50	
	D56	D58	D62	D63	D54	D55	D51	D60
10	42.	52.	40.	48.	47.	53.	43.	44.
40	33.	40.	33.	37.	37.	40.	27.	23.
70	30.	35.	25.	27.	22.	23.	23.	20.
100	20.	25.	16.	14.	16.	15.	12.	12.
130	14.	22.	12.	11.	12.	12.	6.	11.
160	18.	13.	10.6	10.5	12.	10.	8.	6.5
190	12.	13.	8.	9.	7.5	7.	4.	5.3
220	8.7	6.5	5.5	5.5	5.	3.	3.	3.
250	5.	6.0	4.	4.	3.5	3.5	1.3	1.5
280	4.	-	5.	4.	2.8	2.7	0.8	1.2

Table II: Particulate volume vs time data for various experiments with different degrees of air motion performed in a chamber with oiled walls. The tabulated values are $10^6/n$ cc.⁻¹.

t	V = 0		V = 11				V = 40	
	W80		W78		W79		W81	
	obs	calc	obs	calc	obs	calc	obs	calc
5	2.4	3.0	2.5	2.9	2.9	3.0	2.5	2.6
30	4.3	4.1	4.1	4.1	4.1	4.0	4.5	4.5
60	5.6	5.3	5.9	5.6	6.7	5.5	7.7	7.2
90	7.1	6.7	7.5	7.3	7.9	7.3	10.5	10.7
120	8.0	8.0	9.8	9.7	9.0	9.3	13.3	15.1
150	9.7	9.6	11.1	12.0	11.8	11.9	20.	21.
180	11.3	11.1	14.2	15.0	15.7	14.8	28.	29.
210	12.9	13.2	19.	19.	18.3	18.0	39.	39.
240	16.5	15.3	22.	23.	23.	22.	48.	51.
270	16.8	17.7	27.	28.	25.	27.	63.	67.
300	20.	20.	32.	34.	33.	33.	90.	88.
330	26.	23.	41.	41.	-	-	-	-

Table IIa: Mass concentration vs time data for the experiments in table II. The tabulated values are m in mg/m^3 .

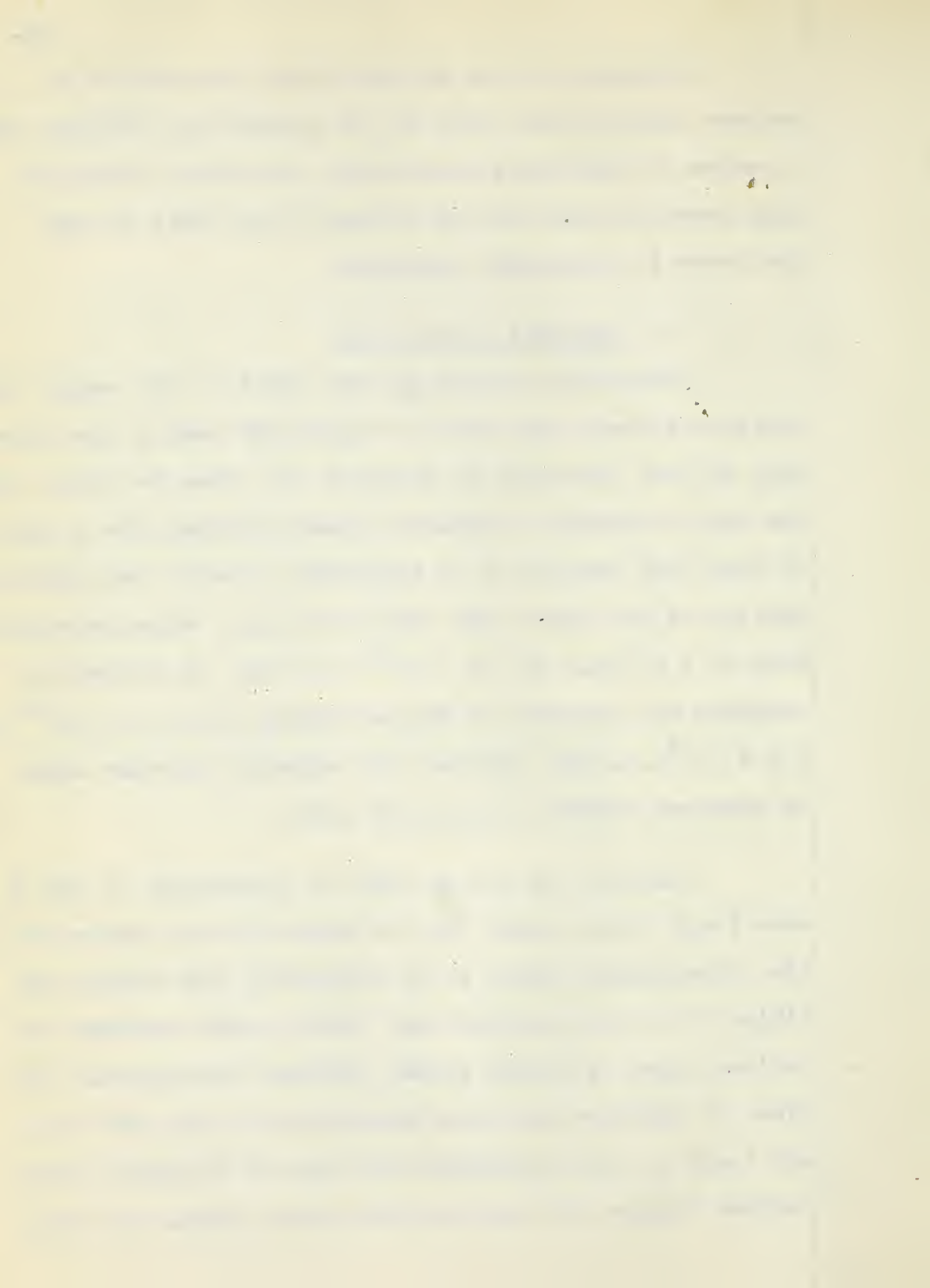
t	V=0	11		40
	W30	W78	W79	W81
10	40.	44.	44.	42.
40	34.	30.	31.	23.
70	28.	28.	28.	15.
100	27.	22.	23.	14.
130	24.	18.	19.	10.
160	25.	16.	18.	9.
190	21.	13.	15.	6.
220	18.	10.	11.	3.3
250	18.	9.0	10.	2.5
280	17.	8.0	9.0	-

Estimates of the particle size distribution at various times in the lives of the aerosols, as obtained in a series of subsidiary experiments, are shown in fig. 12. Each curve is based on the average of two sets of data that were in acceptable agreement.

4. Analysis of the Data.

Particulate volume vs time plots in the manner of previous workers are shown in fig. 13, for some of the data. They are not described by equation (1). Even for still air the curve exhibits a concavity upward, although for a period of about 200 minutes it is acceptably linear. The initial portion of the curve (for still air) has a slope, corresponding to a K value of 5.1×10^{-8} c.c./min. as defined by equation (1), compared to values ranging from 3.0×10^{-8} to 7.9×10^{-8} c.c./min. obtained for ammonium chloride smoke by previous workers (6, 10, 11, 16 p. 46).

Plots of $\log(m)$ vs time as illustrated in fig. 14 were found to be linear for all degrees of air motion over the investigated range. It is noteworthy that Watson and Kibler (14) have reported that Tyndall meter readings for various types of fanned smokes decrease exponentially with time. In addition some mass concentration data for still air found in the literature, when plotted similarly, provide further support. Not only are the plots linear but their



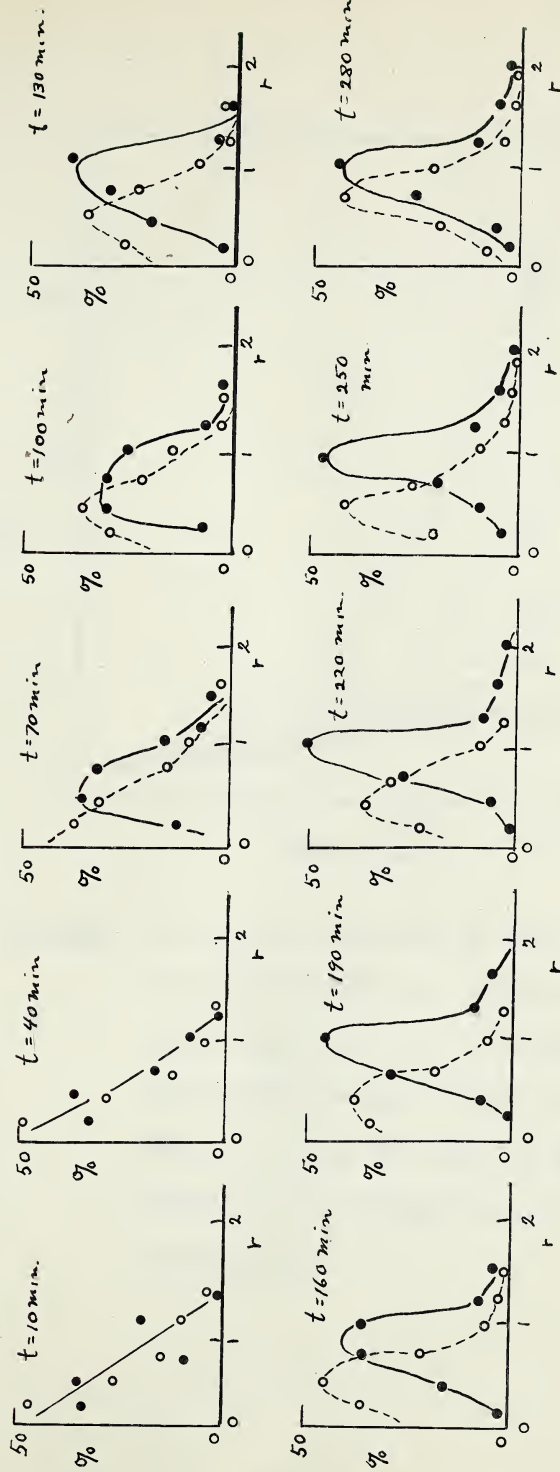


Fig. 12: Estimated particle size distributions. The symbols

● and ○ are associated respectively with V values of 0 and 50 m/min. The ordinate refers to the frequency expressed as a percentage, and the abscissa to the apparent radius in microns.

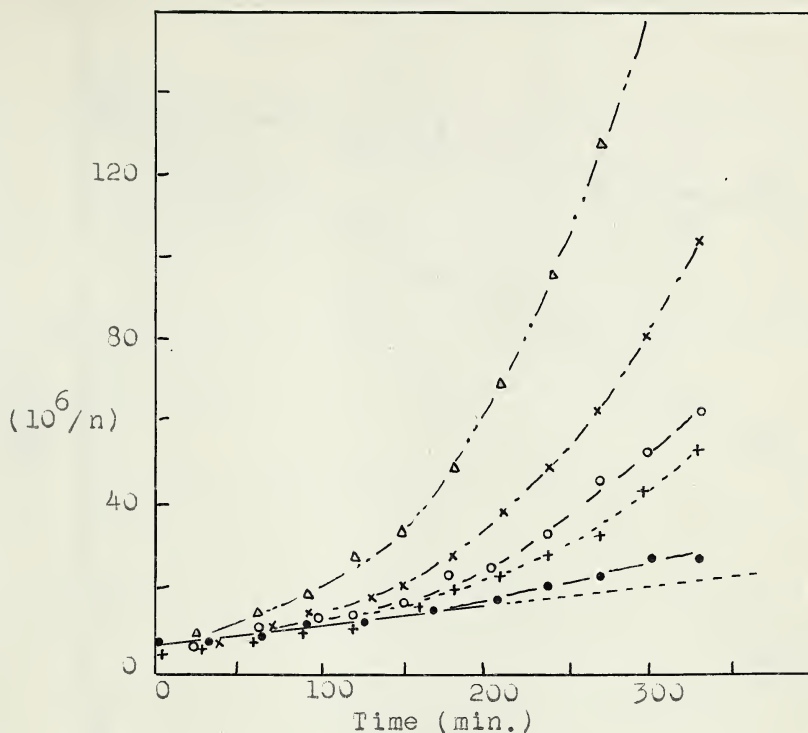


Fig.13: Particulate volume vs time plots for various degrees of air motion. The symbols \bullet , $+$, \circ , \times , and Δ , are associated respectively with V values of 0, 11, 29, 35, and 50 m/min. Each point is an average value for two experiments.

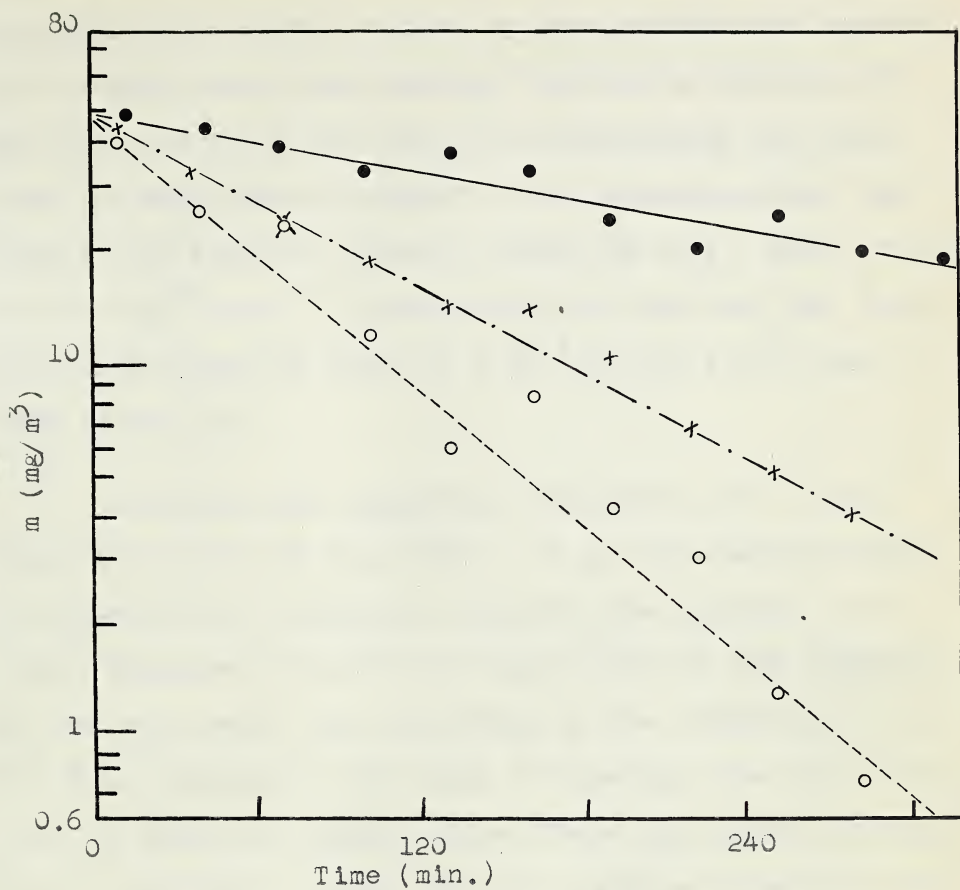


Fig.14: Log mass concentration vs time plots for various degrees of air motion. The symbols ● , + , and ○ , are associated with V values of 0, 11, and 50 m/min. The plotted points represent single determinations.

slopes are strikingly similar. For example the data for two zinc oxide smokes studied by Whytlaw-Gray and Speakman (17) yield a 'mass loss constant' (defined by equation (2) and (3)) of $3.6 \times 10^{-3} \text{ min.}^{-1}$ on disregarding the first point in each which is stated to be erroneous, while some data for an ammonium chloride smoke (16 p.19) give a value of $3.0 \times 10^{-3} \text{ min.}^{-1}$. In comparison our own data for still air yield values of from 3.2×10^{-3} to $3.6 \times 10^{-3} \text{ min.}^{-1}$ (see table III).

Following the suggestion of equation (7) it was found that plots of $\log (10^6/n + E)$ vs time became linear on selection of a suitable value for the constant E by trial. Examples are shown in figs 15 and 16. The linearity of the curve was a fair criterion of the suitability of E for data associated with large V values, but was less critical for plots of smaller slope. Under the worst conditions (still air data) a value of 6 or 7 produced linearity (fig. 16), but higher values did not result in a noticeable concavity upward such as shown in fig. 15. In these circumstances a value of E was selected to produce linearity and to be consistent with other features to appear later. The loss constant β was calculated from the slopes of the curves, and the coagulation constant k ^{from} the values of E and β (see equation 7). The values of the constants for the entire data are given in table III.

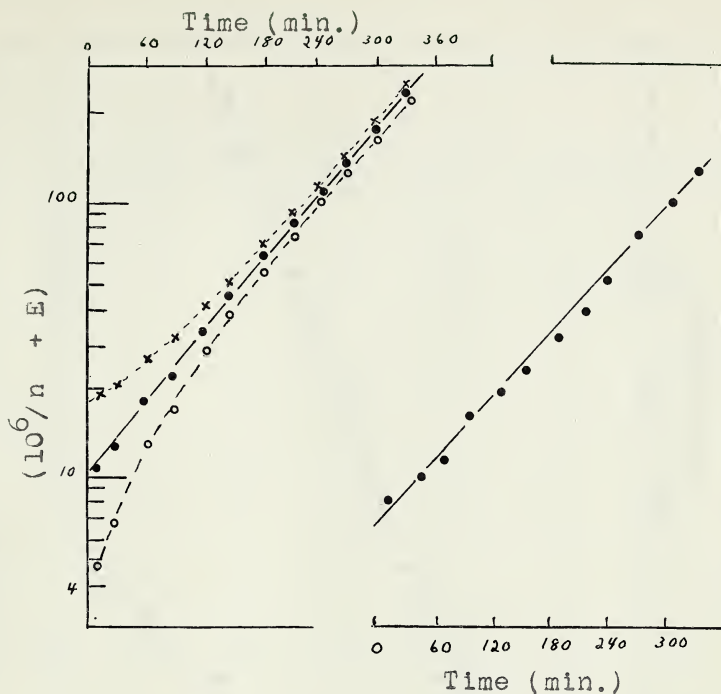


Fig.15: To illustrate the linearity of $\ln(10^6/n + E)$ vs time. The plot at the left with abscissa values at the top is for experiment D51 ($V=50$ m/min.). The symbols o, ●, and x, are associated respectively with E values of 0, 6, and 15. The plot at the right with abscissa values at the bottom is for experiment D62 ($V=35$ m/min.) using an E value of 4.

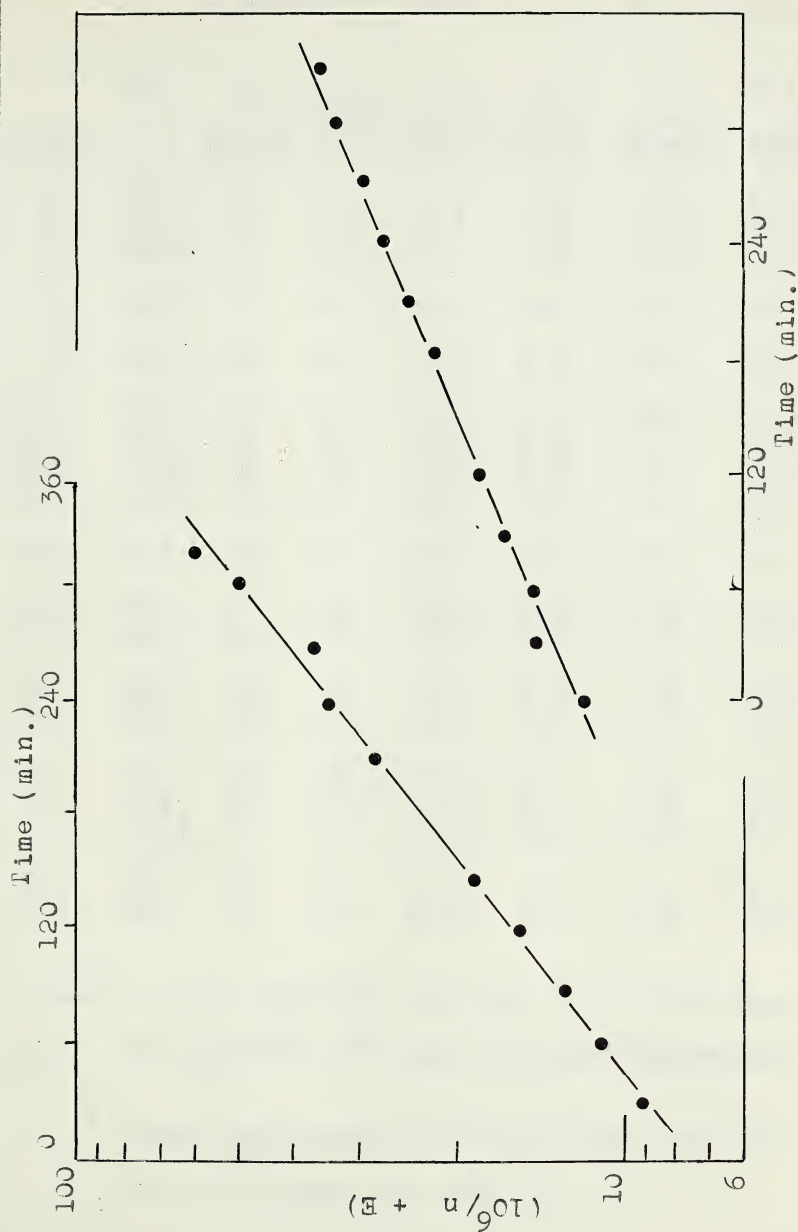


Fig. 16: A companion graph to fig. 15. The plot at the left is for experiment D76 ($V=11$ m/min.), and that at the right is for experiment D40 ($V=0$ m/min.)

Table III: A summary of the experimental values of the constants in equation (5) and equation (7).

V	Exp.	m_0	n_0	α	β	k	k/β	$\frac{\alpha}{E}$
m/min.		mg/m^3	$\times 10^{-4} \text{ cc}^{-1}$	$\times 10^{-3} \text{ min}^{-1}$	$\times 10^{-3} \text{ min}^{-1}$	$\times 10 \text{ cc/min}$	$\times 10^6$	
0.0	D38	39	18	3.2	3.0	2.1	7.0	1.1
0.0	D40	49	19	3.4	3.3	2.3	7.0	1.0
0.0	W80*	41	33	3.6	3.3	2.3	7.0	1.1 ⁴
1.1	D75	47	29	5.2	4.4	2.2	5.0	1.2
5.4	D74	43	40	6.2	5.5	2.8	5.0	1.1
11.	D76	45	31	6.3	6.4	2.6	4.0	1.3
11.	D77	47	24	7.4	5.8	2.3	4.0	1.3
11.	W78*	45	36	6.8	5.8	2.3	4.0	1.2
11.	W79*	45	34	6.2	5.5	2.2	4.0	1.1
22.	D73	48	23	9.0	6.2	3.1	5.0	1.4
29.	D56	47	23	8.1	6.4	3.2	5.0	1.3
29.	D53	60	32	8.5	6.9	2.8	4.0	1.2
35.	D62	43	33	9.6	8.3	3.3	4.0	1.2
35.	D63	48	24	9.6	7.6	3.3	5.0	1.3
40.	D54	52	18	10.8	9.0	3.6	4.0	1.2
40.	D55	56	22	11.0	8.7	4.3	5.0	1.3
40.	W81*	40	42	10.8	8.3	4.3	5.0	1.3
50.	D51	49	26	14.0	9.7	5.8	5.0	1.4
50.	D60	47	25	12.8	9.9	4.9	5.0	1.3

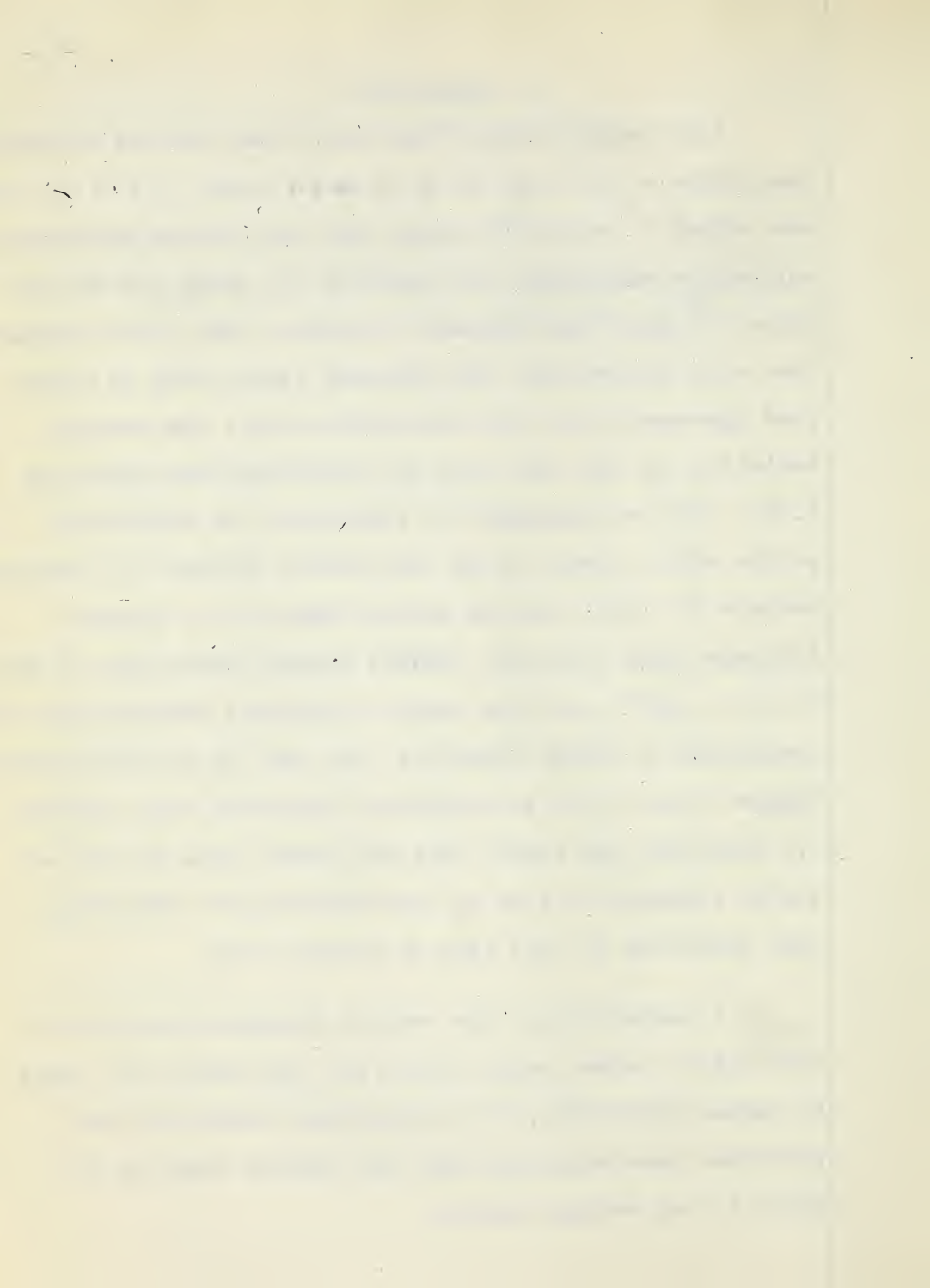
m_0 and n_0 were obtained from the $t = 0$ intercepts of $\log(m)$ vs t , and $\log(10^6/n + E)$ vs t curves respectively.

* These experiments were performed with the walls of the chamber wet with oil.

5. Discussion

Plots such as fig.15 and fig.16 may give an erroneous impression of the experimental scatter since a constant has been added to each $10^6/n$ value. For this reason particulate volumes as calculated from equation (7) using the data of table III have been included in tables I and II for comparison with observation. The observed values were in fairly good agreement with the calculated values; the average deviation for the more than 200 determinations given was 6.2%. This is comparable to the scatter of determined points about linear $1/n$ vs time curves obtained by previous workers for still air and ageing times of 100 minutes. Published data (10,6,11) exhibit average deviations of about 5%, 4%, and 7%, and the overall frequency distribution of deviations is almost identical with that of the data given tables I and II. It is considered therefore that equation (7) describes the entire particle number data as well as may be expected in view of the difficulty of obtaining high precision in this type of aerosol work.

A comparison of the results obtained with dry and with oiled chamber walls (fig.17,18, and table III) shows no marked difference. It is considered therefore that particles once deposited were not removed from the dry walls to any serious extent.



Applications of equation (7) to the data for still air yield a value of 2.2×10^{-7} c.c./min. for the constant k (table III). The Smolochowski coagulation constant for an ideal aerosol as calculated from equation (14) is 1.9×10^{-8} c.c./min. for particles of 1 micron radius and 2.1×10^{-8} c.c./min. for particles of 0.5 microns radius. (See fig. 12) As previously stated the value of K of equation (1) obtained from the early portion of $1/n$ vs time plots was 5.1×10^{-8} c.c./min. in agreement with the results of previous investigators.

For a homogeneous aerosol the ratio of α/β should be unity (equation 10). For a non-homogeneous aerosol loss of the heavier particles must be favored - in sedimentation when the air is still, and in deflections of air currents at surfaces when the air is in motion. Hence α/β should be greater than unity, but perhaps not so very much so, if the particle size range is small. Furthermore, both α and β may be expected to increase with ^{the} rate at which air is brought into contact with surfaces, and if the particle size distribution is not much altered (cf. fig. 12), they should do so in roughly the same proportion. Both these features are characteristic of the data. It is shown in fig. 17 that β is quite closely proportional to α regardless of the degree of air motion. It is shown in table III that the ratio α/β is somewhat greater than unity. These facts

provide strong support for the ideas advanced previously, since β was determined analytically from particle number data, and α directly from an entirely independent set of mass concentration data.

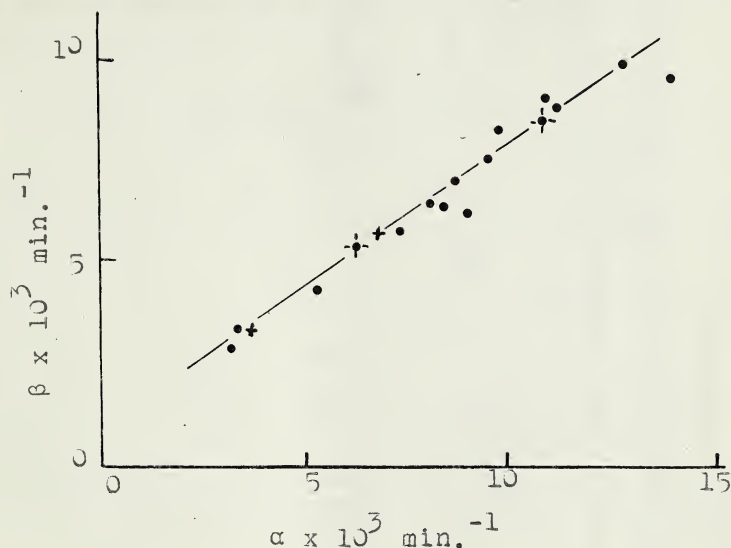


Fig.17: To illustrate the similarity in the increases in α and β with increasing degree of air motion. The symbols •, and +, refer respectively to data obtained with dry and oiled chamber walls.

Increased air motion is accompanied by an increase in the chance of collision of particles with one another, and in the chance of impact of particles on surfaces. Hence k , α , and β may be expected to increase as the degree of air motion becomes greater. The manner in which they do is illustrated graphically in fig.18 in which V (m/min.) is used

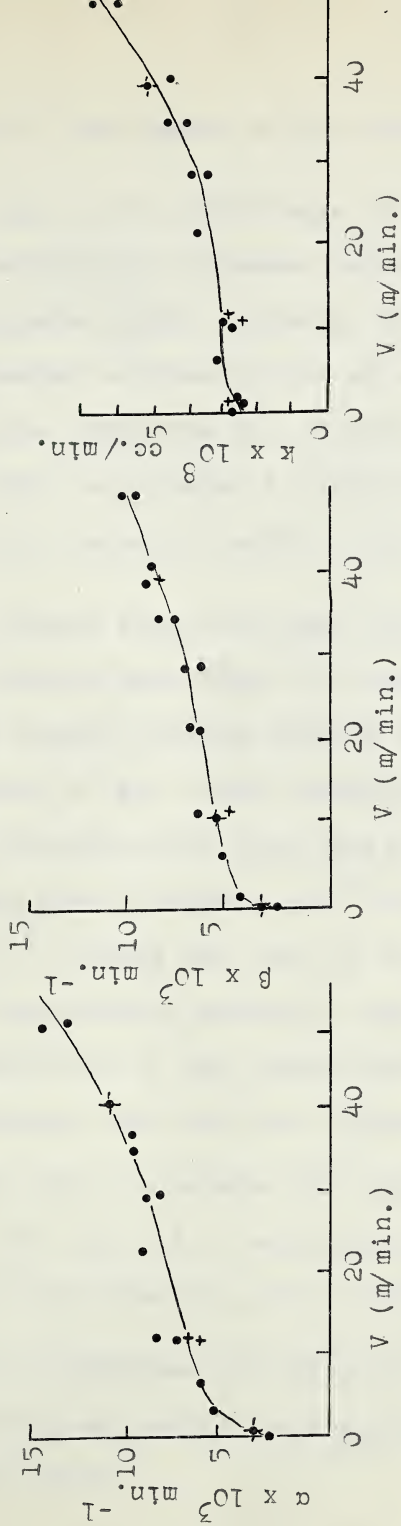


Fig.18: Changes in α , β , and k , with increasing air motion. The symbols \bullet , and $+$, refer respectively to data obtained with dry and oiled chamber walls (table III).

as an index of the degree of air motion.

In view of the wide range of conditions investigated a purely fortuituous agreement between the equations and the data appears highly unlikely. The equations must be regarded however as descriptive of a special case, i.e. that for which time variation in α , β , and k , may be disregarded. They would not be expected to apply, without modification, for example, to aerosols having a much smaller particle size.

It follows from the ideas contained in section 2 that the relative importance of coagulation and surface loss in the ageing process depends strongly on conditions. The importance of the former mechanism should be relatively great for particles with high particle number since the rate of coagulation depends on n^2 while the rate of loss depends on n^* . During the life of an aerosol the relative importance continually shifts to favor the latter mechanism. For the conditions of the experiments described, the rates of disappearance and the total numbers removed by each mechanism have been calculated for hypothetical aerosols (table IV) with the aid of equations 3, 4, 7, 8, and with constants as read from fig. 13. It has been assumed that

(OVER) →

* In general, previous investigators have worked with aerosols having an initial particle number several times that of our smokes.

Table IV: (continued)

		Air speed 25 m/min.				Air speed 50 m/min.			
Init. no. (x 10)	Time (min)	Rates *		gone by		Rates *		gone by	
		Coag	Loss	Coag	Loss	left	Coag	Loss	Coag
10	0	100	290	660	0	0	100	540	980
	30	76	168	500	6	18	65	228	638
	100	43	53	282	12	45	28	44	278
	300	10	3	67	17	73	4	0.7	34
20	0	100	1160	1320	0	0	100	2160	1960
	30	71	581	939	12	17	58	715	1130
	100	37	156	483	24	40	23	110	440
	300	8	7	105	28	64	3	1.5	51
40	0	100	4650	2640	0	0	100	8640	3920
	30	62	1770	1630	22	16	47	1910	1840
	100	28	370	745	37	35	16	222	630
	300	6	14	146	42	52	2	2.6	68
80	0	100	13600	5280	0	0	100	34500	7840
	30	50	4700	2660	36	14	35	4110	2700
	100	19	700	1020	52	29	10	358	800
	300	4	23	185	57	40	1	3.6	81

* Instantaneous rates of coagulation (and loss) in number/cc/min.

the constants hold for smokes with initial n values as low as 10^5 cc.^{-1} and as high as $8 \times 10^5 \text{ cc.}^{-1}$; the experimental data cover the range 2×10^5 to $4 \times 10^5 \text{ cc.}^{-1}$. The data of table IV illustrates the preceding predictions. It indicates that the coagulation process should be of greater relative importance than the surface loss mechanism initially in all experiments where the initial particle number was greater than about $3 \times 10^5 \text{ cc.}^{-1}$. Although for such aerosols the effect of both the coagulation process and the surface loss mechanism decrease with time, they do so in such a manner that the loss mechanism is the major factor after 5.5 hours. For aerosols with low initial particle number (less than $2 \times 10^5 \text{ cc.}^{-1}$) the surface loss mechanism should always be more effective than coagulation. Furthermore it becomes relatively more important as these aerosols age. Table IV also indicates the increase in the coagulation and surface effects with higher degrees of air motion. (It should be noted that the figures quoted above may be expected to apply only for aerosols having particle size distributions comparable to those obtaining in the experiments described in this thesis.)

Aknowledgements.

The results reported in this thesis were obtained under the direction of Dr.G.O.Langstroth. His enthusiastic supervision of the research and his assistance in the organization of the results are greatly appreciated.

I should like to express my thanks to Mr.F.Gleave for his help with apparatus at various times. In particular we are indepted to him for blowing a dozen electrical precipitator tubes.

I should also like to thank Mr.A.J.Stephenson and Mr.J.M.Olyan for assistance with some of the experiments.

References.

1. Carslaw, H. S. "Introduction to the Mathematical Theory of Heat Conduction in Solids" Dover publications, New York, 2nd ed., 1945.
2. Chandrasekhar, S. Rev. Mod. Physics, 15, 1-89, 1943.
3. Drinker, P, and Hatch, T, F. "Industrial Dust", McGraw-Hill Co. New York and London, 1936.
4. Drinker, P, Thompson, R. M, and Finn, J. L. Journal of Ind. Hyg. 8, 307 - 313, 1926.
5. Fuchs, N. Acta Physicochimica, 3, 819-826, 1936.
6. Green, H. L. Phil. Mag. 4, 1046-1069, 1927.
7. Green, H. L, and Watson, H. H. Medical Research Council Special Report 199, H. M. S. O., 1935.
8. Harper, W. R. Trans. Faraday Soc. 32, 1139-1144, 1936.
9. Millikan, R. A. "Electrons, Protons, Photons, Neutrons, and Cosmic Rays."
10. Nonhebel, G. Colvin, J., Patterson, H. S., and Whytlaw-Gray, R. Proc. Roy. Soc. A, 116, 502-522, 1929.
11. Patterson, H. S., Whytlaw-Gray, R, and Cawood, W. Proc. Roy. Soc. A, 124, 502-522, 1929.
12. Tolman, R. C., Vleit, E. B., Pierce, W. McG., and Dougherty, R. H. Journal Am. Chem. Soc. 41, 304-312, 1919.
13. Various authors, "Disperse Systems in Gases", Trans. Far. Soc. 32, 1342-1300, 1936.

14. Watson, P.D., and Kibler, A.I. Jour. Phy. Chem., 35, 1074-1090.
1931.
15. Whytlaw-Gray, R. Jour. Chem. Soc., Pt. I, 268-280, 1935.
16. Whytlaw-Gray, R., and Patterson, H.S. "Smoke", Arnold and
Co., London, 1932.
17. Whytlaw-Gray, R., and Speakman, J.B. Proc. Roy. Soc. A, 102,
615-627, 1923.

Appendix I.

Diffusion as a Mechanism of Loss in Still Air.

As has been stated in section 1, some idea of the importance of diffusion as a loss mechanism in the ageing of an aerosol under still air conditions may be gained from a consideration of the diffusion of homogeneous non-coagulating particles to the walls of a spherical chamber of radius ρ in the absence of gravity. Assuming that the particles striking the walls stick to them, and denoting the diffusion coefficient by D , the distance from the chamber center by ρ , and the number of particles per c.c. by n , the situation is described by,

$$\frac{\partial (n\rho)}{\partial t} = D \frac{\partial^2 (n\rho)}{\partial \rho^2} \quad \text{--- (1)}$$

$$t = 0 \quad n = n_0 \quad 0 < \rho < \rho_0 \quad \text{--- (2)}$$

$$\rho = \rho_0 \quad n = 0 \quad \text{for any value of } t \quad \text{--- (3)}$$

The solution is as follows;

$$\text{Let } n\rho = X(\rho)Y(t) \quad \text{--- (4)}$$

$$XY' = DX''Y$$

Therefore $Y'/Y = DX''/X = k$

and hence

$$Y' - kY = 0 \quad \text{--- (5)a}$$

$$X'' - (k/D)X = 0 \quad \text{--- (5)b}$$

Hence $n = e^{kt} (c_3 \sin \sqrt{-k/D} \rho + c_4 \cos \sqrt{-k/D} \rho)$ for $k < 0$

From (2) $c_4 = 0$

From (3) $c_3 \sin \sqrt{-k/D} \rho_0 = 0$

this requires $\sqrt{-k/D} \rho_0 = \ell \pi$ where ℓ is an integer.

i.e. $k = \frac{-\ell^2 \pi^2 D}{\rho_0^2}$

Hence

$$n\rho = c_3 e^{\frac{-\ell^2 \pi^2 D t}{\rho_0^2}} \sin \frac{\ell \pi \rho}{\rho_0}$$

The solution for the range $0 < \rho < \rho_0$

must be

$$n\rho = \sum_{\ell} A_{\ell} e^{\frac{-\ell^2 \pi^2 D t}{\rho_0^2}}$$

Hence at $t = 0$

$$n_0 \rho = \sum_{\ell} A_{\ell} \sin \frac{\ell \pi \rho}{\rho_0} \quad \text{--- (7)}$$

In order to determine the values for the coefficients A_{ℓ}

we equate the right hand side of equation (7) to the

Fourier sine series for n_0 for the range $0 < \rho < \rho_0$

$$\begin{aligned} \text{i.e. } \frac{n_0 \rho_0}{\pi} \left[\sin \frac{\pi \rho}{\rho_0} - \frac{1}{2} \sin \frac{2\pi \rho}{\rho_0} + \frac{1}{3} \sin \frac{3\pi \rho}{\rho_0} - \dots \right] \\ = \sum A_{\ell} \sin \frac{\ell \pi \rho}{\rho_0} \end{aligned}$$

Hence equating coefficients we have,

$$A_{\ell} = \frac{(-1)^{\ell+1}}{\ell} \frac{2n_0 \rho_0}{\pi}$$

Substituting this value of A_{ℓ} in equation (6) it follows

that

$$n = \frac{2n_0 \rho_0}{\pi \rho} \sum_{\ell} \frac{(-1)^{\ell+1}}{\ell} e^{-\frac{\ell^2 \pi^2 D t}{\rho_0^2}} \sin \frac{\ell \pi \rho}{\rho_0} \quad (8)$$

where ℓ takes on successive integral values. The fraction F of particles left at time t is given by volume integration as follows.

$$\begin{aligned} F &= \frac{2n_0 \rho_0}{\pi} \cdot \frac{2}{\left(\frac{4}{3}\pi n_0 \rho_0^3\right)} \int_0^{\rho_0} \int_0^{2\pi} \int_0^{\frac{\pi}{2}} \sum_{\ell} \frac{(-1)^{\ell+1}}{\ell} e^{-\frac{\ell^2 \pi^2 D t}{\rho_0^2}} \rho \sin \frac{\ell \pi \rho}{\rho_0} \sin \theta \, d\theta \, d\phi \, d\rho \\ &= \frac{6}{\pi^3} \left\{ \sum_{\ell} e^{-\frac{\ell^2 \pi^2 D t}{\rho_0^2}} \frac{(-1)^{\ell+1}}{\ell^2} \frac{2(\ell+1)}{\pi} \right\} \\ &= \frac{6}{\pi^2} \sum_{\ell} \frac{1}{\ell^2} e^{-\frac{\ell^2 \pi^2 D t}{\rho_0^2}} \end{aligned}$$

Appendix II

Measurement of the Degree of Air Motion.

In order to specify the degree of air motion in the preceding experiments it was necessary to determine some factor descriptive of it. Under completely chaotic conditions, the amount of air passing through any given small volume in unit time, regardless of direction, would be a suitable index of the degree of air motion. The various anemometers described in the literature are unsuitable for the determination of this quantity, since those of the mechanical type measure the vector sum of air velocities, and those of the hot wire or thermocouple type give readings dependent to some extent on the direction of the air flow past them. The instrument developed to measure the desired quantity in the preceding experiments

in the preceding experiments has practically non-directional properties. It is based on the heated thermocouple principle. The design and characteristics are outlined below.

Design of the Instrument.

Six identical heating coils were wound on short aluminum tubes located at equal distances from the origin on the X Y Z axes of a Cartesian coordinate system as indicated in fig. 19, 20(a). Each coil consisted of ten turns of number 34 B and S oxide coated nichrome wire. The coils were connected in series and had a total resistance of 12 ohms.

A thermocouple arrangement consisting of six 'hot' junctions in parallel and a common 'cold' junction was constructed from number 31 B and S copper wire and number 30 B and S constantan wire as indicated in fig. 20 (b). A 'hot' junction was inserted in each aluminum tube, the thermocouple wires serving as supports for the tubes. The common 'cold' junction was located 20 cms. from the center of symmetry of the head shown in figs. 19, 20(a) and remained at room temperature.

A standard current passing through the heating coils caused a temperature difference between the 'hot' and 'cold' junctions. Because of the cooling effect of air flow past the head, the temperature difference (and so the E.M.F. generated by the arrangement) depended on the rate of air flow.



Fig. 19: The instrument used for measuring the time-average air speed. The photograph is 1.9 times the actual size.

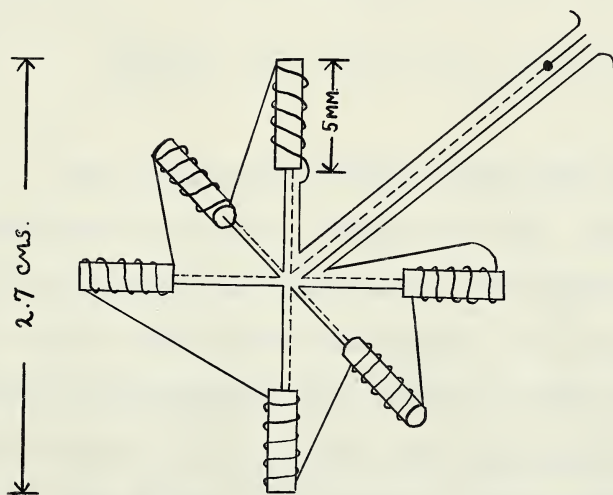


Fig.20 (a):

The instrument head.

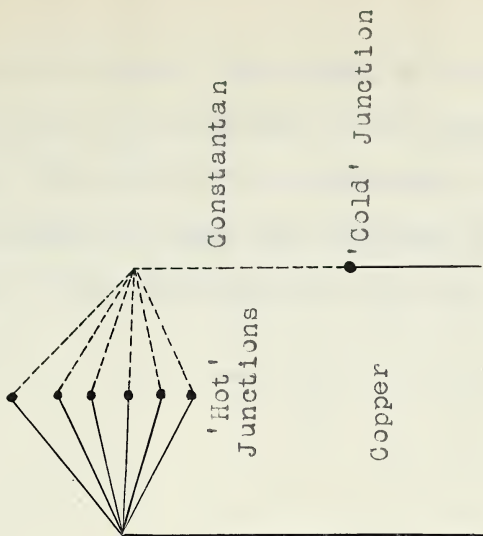


Fig.20 (b):

The thermocouple junctions.

Hence the rate of flow could be determined from the measured E.M.F. with the aid of an appropriate calibration curve. The geometrical arrangement of the heating coils was designed to make the readings of the instrument independent of the direction of air flow.

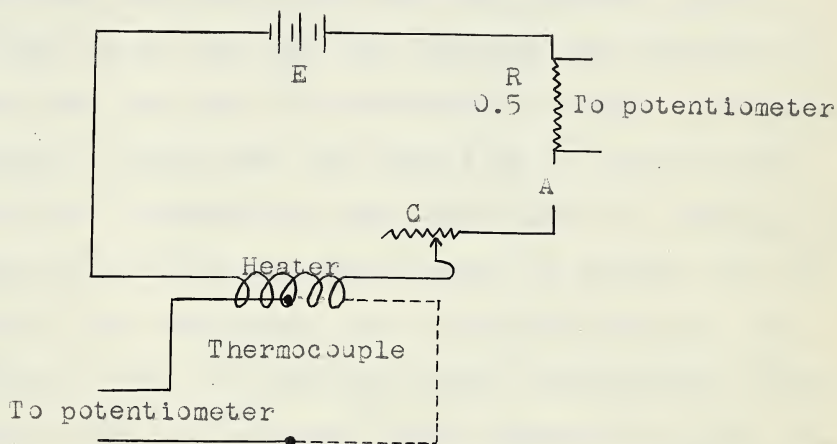


Fig.21: The electrical precipitator.

The electrical circuit used with the instrument is indicated in fig(21). Only one 'hot' thermocouple junction and one heater coil are shown. The heater current from a 6 volt Pb cell E, was controlled by a rheostat C and measured by determining the potential drop across a fixed series resistance R. In practice the heating current was adjusted until the E.M.F. developed by the thermocouples was 950 micro-volts in still air, and was maintained at this value during subsequent measurements.

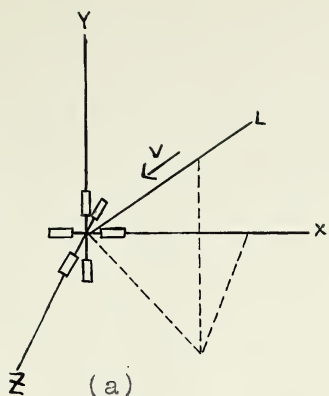
Calibration of the Instrument.

For calibration the instrument was mounted on a revolving arm driven by a motor with a reduction gear system. Electrical connections were made through mercury cups which served as slip rings. The rate of flow of air past the instrument head was calculated from the measured number of revolutions of the arm per unit time, and the distance of the head from the axis of revolution. The speed of rotation was varied in steps over the range 1.86 to 73 revs./min., and the E.M.F. measured at each. The effect of changing the direction of air flow was investigated by varying the orientation of the instrument head on the rotating arm. The directions of the air flow for typical orientations of the instrument head are indicated by the arrows in fig.22. The whole apparatus was enclosed in a 1.12 meter cube to protect it from stray air currents. Typical results are shown in fig.23.

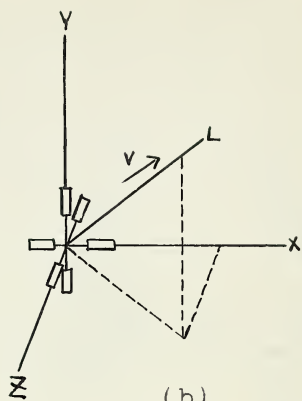
Remarks

Examination of fig.(23) indicates that over the range investigated the readings of the instrument were practically independent of the direction of the air flow past the head.

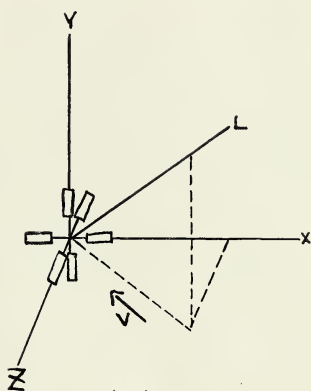
The time lag of the instrument was small. Subsidiary experiments showed that equilibrium was attained within one minute after an abrupt change in air velocity from 12



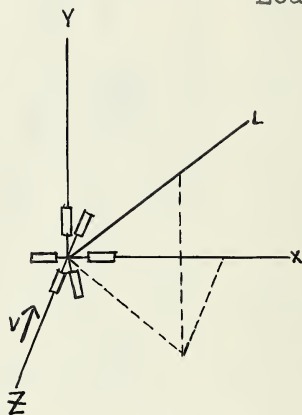
(a)
V parallel to Leads



(b)
V antiparallel to
Leads



(c)
V at 45 degrees to Z axis
in XZ plane.



(d)
V parallel to X, Y, or Z
axis.

Fig.22: The directions of air flow for typical orientations of the instrument head during calibration. In all cases the leads make equal angles with the X, Y, and Z axes.

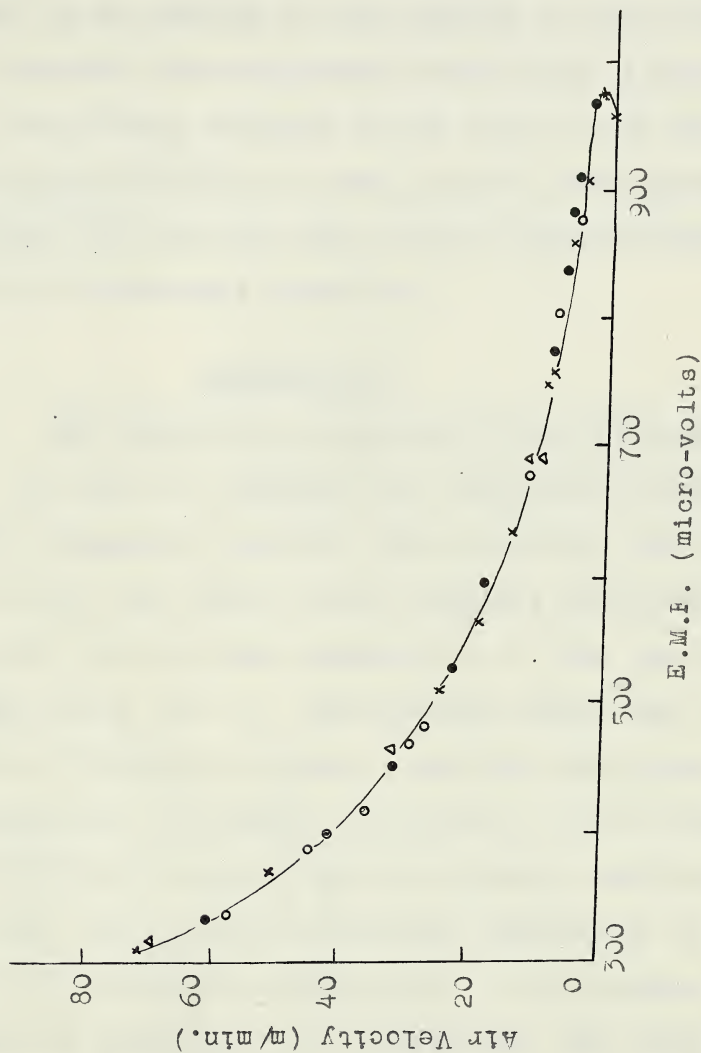


Fig. 23: The calibration curve. The symbols ●, ×, ○, and Δ, refer respectively to directions of air flow "a", "b", "c", and "d" as indicated in fig. 22.

meters per minute to 46 meters per minute.

During development work instruments of various designs, including single coil types, were tested and were found to be unsuited to the purpose in mind, either because of excessive time-lag, marked directional properties, or both. In particular, a decrease in the size of the head of the instrument described in this appendix, accomplished by bringing the heating coils closer together, resulted in some loss of directional properties.

Appendix III

The Coagulation Constant for an Ideal Aerosol.

In order to calculate the coagulation constant for an ideal homogeneous aerosol whose spherical particles stick on contact one could use the analysis developed by Smolochowski for the rapid coagulation of sols (see references 10, 16, 8, 2, on page 51). Smolochowski showed that the probability of encounter between a particle and others in its neighborhood is $4\pi Sn(D_1 + D_2)$, where n is the number of particles per c.c., (D_1 is the diffusion coefficient of the particle and D_2 is the diffusion coefficient of the particle with which it collides, and S is the radius of the sphere of collision of two particles. The total number of collisions per unit time is therefore $\frac{1}{2} \cdot 4\pi S(D_1 + D_2)n^2$ so that $k = 2\pi S(D_1 + D_2)$ will be the coagulation constant

defined by equation (5) of section 1. For the collision of two particles both of radius r microns, $S = 2r$, and the relative diffusion coefficient $(D_1 + D_2)$ will be twice the diffusion coefficient for each particle given by equation (12) of section 1. Hence,

$$k = \frac{80 RT}{\pi N} \left(1 + \frac{A\lambda}{r} \right) \text{ cc/min.} \text{ --- (1)}$$

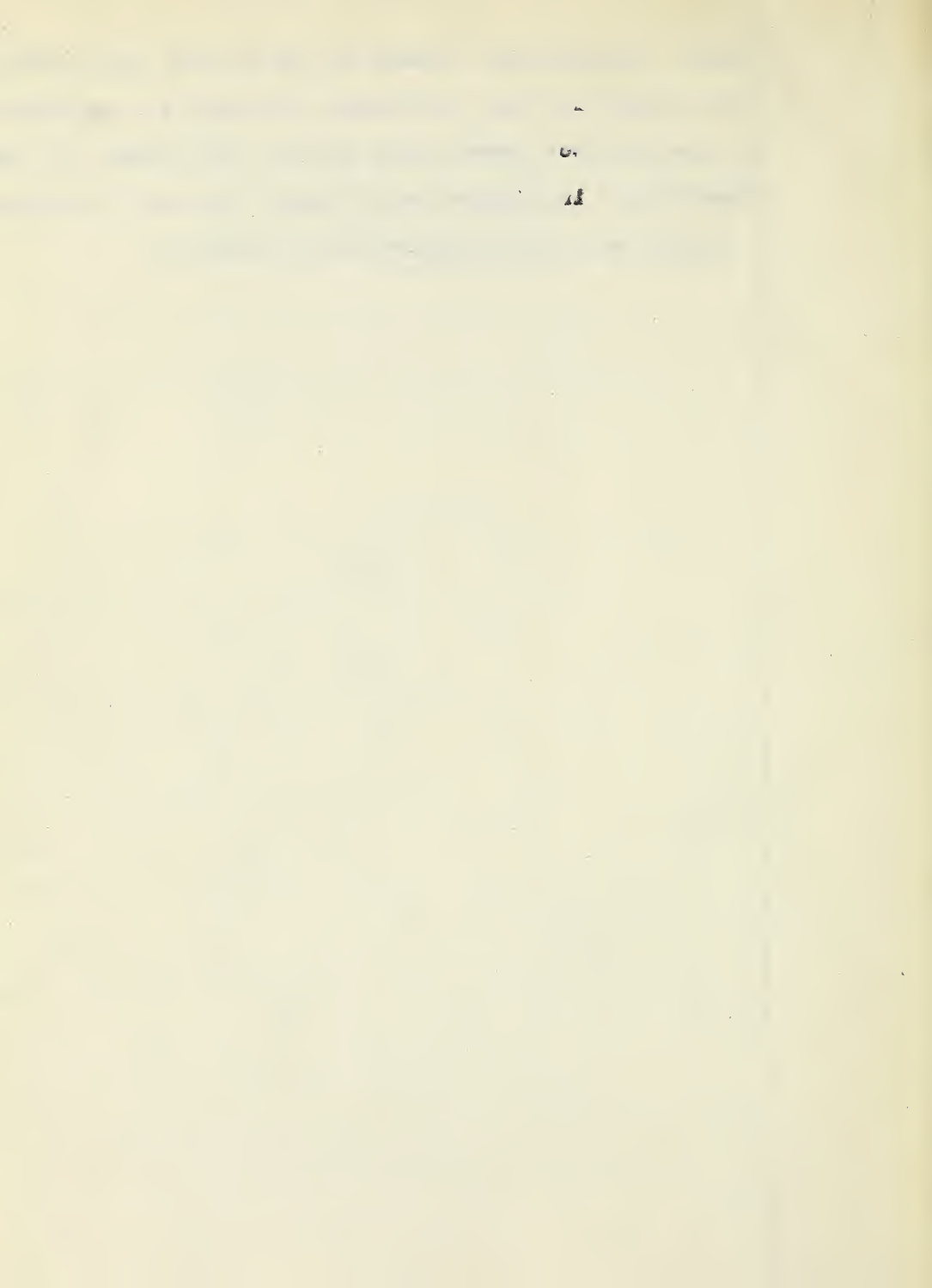
Equation (13) of section 1 was obtained from (1) by the substitution of appropriate constants.

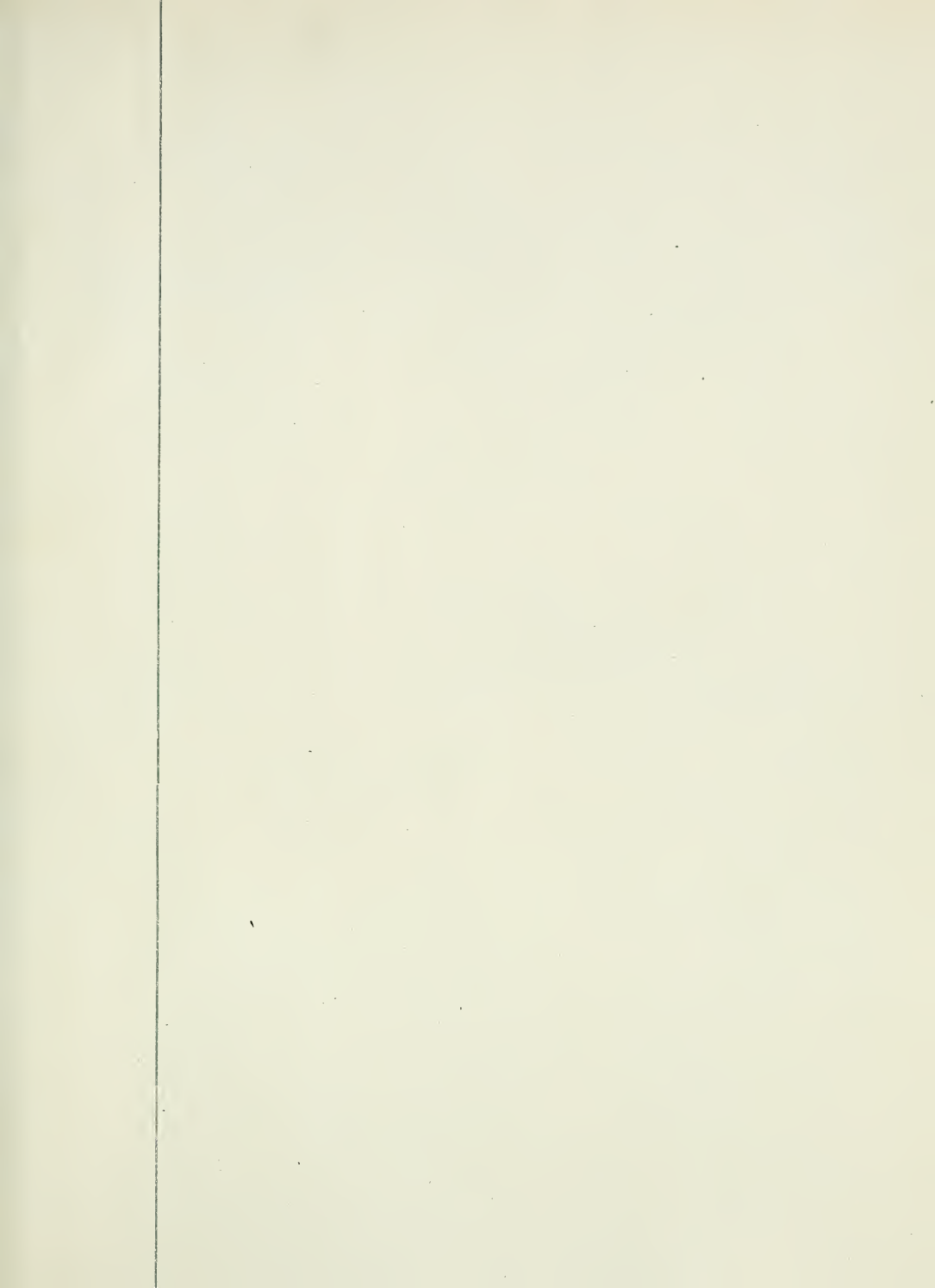
Appendix IV

Analysis of the Mass Concentration Samples.

The mass concentration samples obtained as described in section 2 by dissolving the deposits formed by the electrical precipitator tubes in 50 c.c. of distilled water were each poured into a separate 50 c.c. Nessler tube. These test solutions were analysed for NH_4Cl content by adding 1 c.c. of Nessler's reagent to each of the solutions and to each of a set of freshly prepared standard NH_4Cl solutions contained in 50 c.c. Nessler tubes. After about 10 minutes the yellow color of the test solutions were compared with that of the standards. Although precipitates of 0.002 to 0.040 mg. of NH_4Cl can be detected in this way, most of the results reported above were obtained by using eight standards containing from 0.002 mg. to 0.040 mg. of NH_4Cl .

NH_4Cl . Appropriate volumes of the aerosol were drawn for each sample so that the deposit obtained in the electrical precipitator tubes would fall in this range. It was possible, by interpolation, to detect deposits to within 0.0005 mg. using this method of analysis.





B29754